BILAYER CHITOSAN/ZEIN BASED NANOFIBERS FOR ANTIMICROBIAL WOUND DRESSING APPLICATION

A Thesis Submitted to
the Graduate School of
İzmir Institute of Technology
in Partial Fulfillment of the Requirements for the Degree of

MASTER OF SCIENCE

in Chemical Engineering

by

Nilsu İSKEÇMAN

December 2021

İZMİR

ACKNOWLEDGMENTS

Firstly, I would like to express my sincere gratitude to Prof. Dr. Funda Tıhmınlıoğlu for her supervision, guidance, encouragement, and support throughout my thesis studies.

I would like to thank Tubitak for providing a 2210/C scholarship within the scope of my master's thesis.

I would like to thanks to my lab mate Dr. Sedef Tamburacı, and my friends Burcu Sırma and Damla Yalçın for their help, support, patience, and friendship. Besides, I would like to thank to my co-worker Şebnem Yezdan Yıldız for her motivation, support, friendship and understanding.

I would like to special thanks to my family, Adnan İskeçman, Ayşe İskeçman and Ata İskeçman for their endless support, understanding and patience during my education.

ABSTRACT

BILAYER CHITOSAN/ZEIN BASED NANOFIBERS FOR ANTIMICROBIAL WOUND DRESSING APPLICATION

Nowadays, modern functional wound dressings have become prominence due to their biocompatible, biodegradable, and non-toxic nature and similarity with ECM of skin. Environmentally friendly halloysite nanotubes (HNTs) are gained attention due to their tubular structure that allow encapsulation of various agents into these tubes to enhance antimicrobial activities in a sustained manner as well as with enhanced mechanical properties for the development of antimicrobial nanocomposites. In this thesis, bilayer wound dressing was fabricated by using Zein-Vancomycin loaded HNTs nanofibers as upper layer to mimic ECM of skin and provide antibacterial protection, and chitosan sponge as bottom layer to absorb the excess exudates of wound, provide gas transmission and facilitate the migration of inflammatory and fibroblast cells into the healing wounds. The morphology of nanofibers and encapsulation efficiency of Vancomycin into HNTs are optimized to achieve similar fiber structure with skin tissue, and to obtain sustained release of the drug. Chemical interaction between Vancomycin-HNT and Zein-HNT were characterized by FT-IR. The surface charge of drug loaded and unloaded HNTs was determined by zeta potential analysis. Bilayer sponges were characterized by SEM, FT-IR, porosity, mechanical properties, contact angle, water vapor transmission rate, swelling, degradation, in vitro drug release, and antimicrobial activity analyzes. The diameter of drug loaded HNT-Zein nanofibers were found in the range of native skin collagen fibril (203± 0,05- 225±0,06 nm). The water vapor permeability of the wound dressings is found in the appropriate range for wound healing (2833- 2490 g/m^{2}day). Bilayer dressings containing two different drug:HNTs ratios reached 78% cumulative release at the end of 14 days, however rand the release medium showed antimicrobial activity. In conclusion, the developed drug-loaded bilayer mat has been found as a potential candidate for wound dressings applications to treat the chronic infections.

ÖZET

ANTİMİKROBİYAL YARA ÖRTÜSÜ UYGULAMALARINA YÖNELİK ÇİFT TABAKALI KİTOSAN/ZEİN TEMELLİ NANOELYAFLAR

Günümüzde modern fonksiyonel yara örtüleri, biyolojik olarak uyumlu, parçalanabilen, toksik olmayan ve cildin ECM'sine benzerliği sayesinde ön plana çıkmışlardır. Bu yara örtülerinin mekanik özelliklerini iyileştirmek ve kümülatif ilaç salım sürelerini arttırmak için son zamanlarda çevre dostu halloysit nanotüpler (HNT'ler) tercih edilir. Tübüler yapıları sayesinde ilaç salınımını daha kontrollü hale getirmek için çeşitli ajanlar bu tüplere enkapsüle edilebilmektedir. Bu tezde, cildin ECM'sini taklidi ve antibakteriyel koruma özellikleri nedeniyle üst katman olarak Zein-Vancomycin yüklü HNTs nanofiberleri kullanılmıştır. Ayrıca alt tabaka olarak yaranın fazla eksüdasını absorbe etmesi, gaz geçirgenliği sağlaması için kitosan sünger kullanılmıştır. Bu çalışmada iki katmandan oluşan yara örtüsünün üretilmesi ve karakterize edilmesi amaçlanmıştır. Nanoliflerin morfolojisi, HNT'lerin kapsülleme verimliliği ve kontrollü Vankomisin ilaç salımı optimize edilmiştir. Üst ve alt tabakaların morfolojileri, taramalı elektron mikroskobu (SEM) kullanılarak analiz edilmiştir. Vankomisin-HNT ve Zein-HNT arasındaki kimyasal etkileşim, FT-IR ile karakterize edilmiştir. İlaç yüklü ve yüksüz HNT'lerin yüzey yükleri, zeta potansiyel analizi ile belirlenmiştir. Nanoliflerin ağırlık kaybı yüzdesi, termogravimetrik analiz (TGA) kullanılarak karakterize edilmiştir. Nanolif tabakasının hidrofilik karakterinin değişimi temas açısı ölçümü ile hesaplanmıştır. Çift katmanlı süngerler SEM, FTIR, gözeneklilik, mekanik özellikler, su buharı iletim hızı, şişme, bozunma, kümülatif ilaç salımı, kinetik salım modelleri ve antimikrobiyal aktivite analizleri yapılmıştır. İlaç yüklü HNT-Zein nanoliflerinin çapları ciltteki kollajen fibril aralığında bulunmuştur (203± 0,05- 225±0,06 nm). Yara örtülerinin su buharı geçirgenliği yara iyileşmesi için uygun aralıktadır (2833-2490 g/m^{2}gün). Çift tabakalı pansumanlar 14 günün sonunda %78 kümülatif salıma ulaşılmıştır. Ayrıca antimikrobiyal aktivite tespit edilmiştir. Sonuç olarak, geliştirilen ilaç yüklü çift katmanlı yara örtüsü, yara pansumanları için potansiyel aday olarak bulunmuştur.

TABLE OF CONTENTS

LIST OF FIGURES

Figure **Page**

LIST OF TABLES

CHAPTER 1

INTRODUCTION

The skin is the largest organ in human body which forms nearly 15% of the total adult body weight. It serves many important purposes such as protecting the human body against external physical, chemical and biological attacks, preventing excessive water loss from the body and taking part in thermo regulation process (Kolarsick et al., 2011). Wound is a break of skin tissue that can be occurred due to lots of external damages, accident, injury, or burns. Wound healing which is a natural regeneration of skin defined as a process that begins with trauma and ends with the new tissue formation (Sofokleous et al., 2013). Many various materials have been used from past to today for wound healing. In the past, honey pastes, plant fibers and animal fats were preferred as wound dressing materials, but today, with the discovery of new biopolymers, modern wound dressings are used (Zahedi et al., 2010).

Different kinds of wound dressing materials including synthetic or natural polymers have been used for wound dressing applications, however in recent years, natural polymers such as silk fibroin, alginate, chitosan, collagen, gelatin, zein or pectin have become pointed more than synthetic polymers due to their low toxicity, biodegradability, and biocompatibility with human tissues (Kurtoğlu & Karataş, 2009). Zein is one of the natural or biopolymer which found in corn as a protein and can be called as ‘‘green material’’ due to obtained from renewable source. Zein can be formed as films, microspheres, nanoparticles, micelles, gels, foams, and fibers. However, zein's ease of electrospinning makes it preferred for medical and tissue engineering applications as it resembles and mimics the extracellular matrix of the skin (Kimna et al., 2018). In addition, zein's excellent biocompatibility, biodegradability, resistance to microbial attack, water insolubility and amphiphilic nature make zein special as it provides regularity for various applications. Zein fiber has been used with several synthetic antibacterial drugs such as ketoprofen (Lee et al., 2017), cyclodextrin (Kayaci & Uyar, 2012) , silver sulfadiazine (Ullah et al., 2019) and natural antibacterial agents such as thyme oil (Liu et al., 2019) sesamol (Liu et al., 2019) for wound dressing applications. However, zein has a weak mechanical character and an uncontrolled release of drugs from

the zein matrix. Therefore, it is necessary to use a different material to improve these poor properties of zein (Gorrasi & Vertuccio, 2016).

To achieve and improve strong mechanical property and controlled drug release behavior of zein; some additives or fillers can be used such as plasticizers (e.g., glycerol) or crosslinking agents (e.g., citric acid) (Kimna et al., 2018 ; Dashdorj et al., 2015) . Recently, Halloysite Nanotubes (HNTs) have been used as green inorganic nanofiller to improve the mechanical properties of polymeric materials as well as development of antimicrobial composites. HNTs are abundant, cheap, and non-toxic clay minerals. It has a tubular structure allowing for increased surface area and drug loading inside the tiny tubes to release in specific environment in more controlled manner (Lvov & Abdullayev, 2013). Several antibiotics, anticorrosion agents, essential oils were encapsulated into HNTs such as doxycycline (Feitosa et al., 2014) , vancomycin (Avani et al., 2014) gentamicin (Wali et al., 2019), benzotriazole (BTA) (G. Cui et al., 2020) thyme oil (Lee et al., 2017). According to our knowledge, there is no research study on this drug loaded HNTs in zein polymer matrix. Although single layer nanofiber dressings are compatible with the extra cellular matrix of the skin, recent studies have focused on bilayer/multilayer biomaterials to mimic the different layers of skin consisting of different cell types and to regenerate big wound defects, especially for diabetic patients. Therefore, in this study chitosan sponge which is a natural polymer derived from chitin selected as bottom layer to provide gas transmission bacterial prevention, mechanical support as well as adsorption of high wound exudates due to its high swelling capacity.

The aim of this study, therefore, is to produce bioactive bilayer modern wound dressing which composed of electrospun zein-vancomycin loaded HNTs nanofiber mat as the upper layer that mimics the ECM structure of skin tissue and releases vancomycin antibiotic in a sustained manner and chitosan sponge as the bottom layer produced by freeze drying, is used to collect excess exudates around the wound and also provides mechanical support and ensuring bacterial prevention & gas transmission.

In this thesis firstly, zein, zein-HNT and zein-vancomycin loaded HNT nanofibers were fabricated and characterized by using SEM, FTIR, zeta potential measurement, encapsulation efficiency, thermogravimetric analysis, and contact angle measurements. Effects of HNTs concentration, HNT:drug ratio with varying electrospinning parameters on vancomycin encapsulation efficiency were studied. The upper layer was fabricated with the optimum HNT:drug ratio having highest encapsulation efficiency. The lower chitosan sponge layer was analyzed by SEM and liquid displacement method to determine

the microstructure and % porosity. Bilayer wound dressings were characterized according to their mechanical strength, water vapor permeability, % swelling and degradation cumulative drug release profile, kinetic model, and antibacterial characteristics. In this thesis, it was aimed to fabricate zein-drug loaded HNTs nanofiber as upper layer because of their antibacterial barrier effects with sustained release of vancomycin. The porous bottom layer with high swelling capacity can serve as a wound exudate absorber as well as providing initial cell attachment and facilitating the migration of inflammatory and fibroblast cells into the healing wounds. Bilayer porous wound dressing was designed as modern wound dressing materials for acute wounds.

In Chapter 1 of the thesis, skin structure, wound healing and the aim of the study were explained. Chapter 2 contains literature review on wound dressing materials and wound dressing types and zein based wound dressing studies. Experimental part of the thesis including materials and methods were described in Chapter 3. The results and discussions of the study were given in Chapter 4. Chapter 5 finally gives the conclusion of the thesis.

CHAPTER 2

LITERATURE REVIEW

2.1. Skin and Structural Properties

The largest organ in humans is the skin, with an area of approximately 2 m^2. The skin basically has three functions. Protect the internal organs from microbial invasion and our body from UV radiation, prevent water loss from body and act as a barrier to regulate the body's temperature. In addition to these two functions, the skin also supports the body's immune system and the perception process with our senses. Cells on the surface of the skin are stripped from the upper layers and are constantly replaced by new cells found in the inner layers. The skin has three different layers which are shown in Figure 2. 1. These layers are epidermis, dermis and hypodermis which are self-renewing layers with various functions (Ghomi et al., 2019).

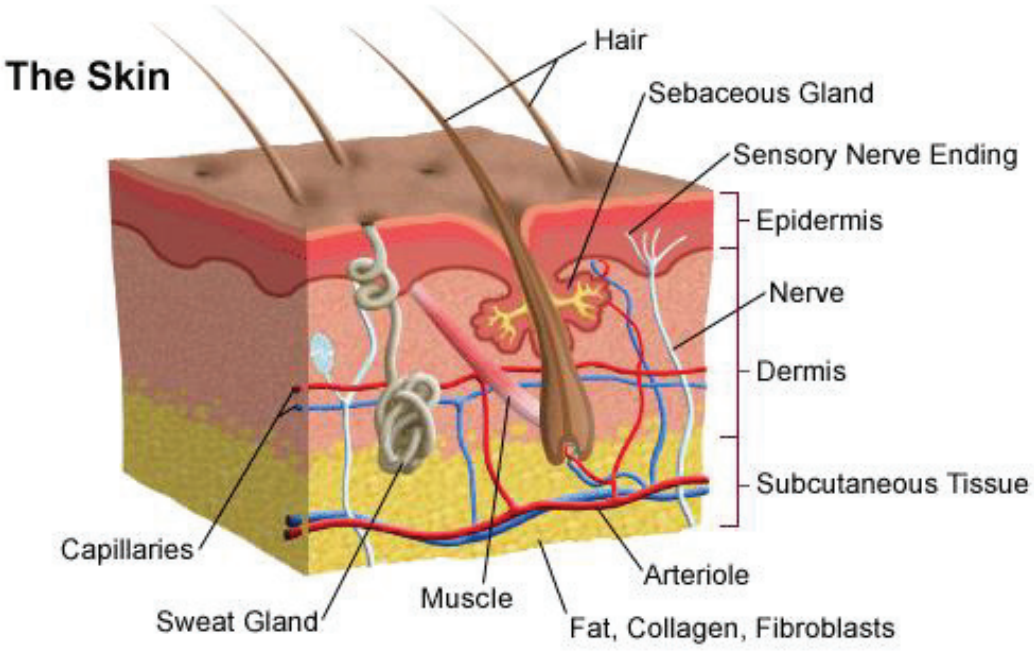

Figure 2. 1. Representation of skin layers

(Source: Losquadro, 2017)

2.1.1.Epidermis

The epidermis is the top layer of the skin. For this reason, it directly protects people from external factors or impacts. The epidermis is the layer responsible for the color, texture and moisture of the skin. It is a layer of skin that is constantly renewed and therefore gives rise to derivative structures such as nails, pilosebaceous apparatus pilosebaceous apparatuses, nails, and sweat glands. The epidermis consists of 4 layers which are listed below respectively from outside to inside of skin.

- Stratum corneum
- Stratum granulose
- Stratum spinosum
- Stratum basale

Cells in the outermost layer of the epidermis gradually lose their organelles and become more compact and they form the stratum corneum. Stratum granulosum lost the ability to cell division and consists of flattened keratinocytes. The stratum spinosum layer consists of keratinocytes synthesizing keratin and their cellular proliferation capacity is limited. The inner layer just above the dermis is the stratum basale. This layer consists of basal cells that produce new skin cells, Merkel cells that transmit sensations to the nerves, and melanocytes that give the skin its natural color (Kolarsick et al., 2011).

2.1.2. Dermis

The dermis is the second layer of the skin and is located just below the epidermal layer. The thickness of the dermis layer varies according to the body region which includes intercellular support tissue and fibroblast cells, among them nerve, vessel, lymphatic structures, sebaceous glands, nail and hair follicles. The main component of the dermis is collagen. Collagen is an important structural protein of the skin that is resistant to stress, but it is not very effective against deformation and tearing of the skin. The dermis layer provides the skin's flexibility, elasticity and compression strength which protects body from mechanical injuries and helps the thermal regulation. The dermis interacts with the epidermis and provides cooperation between tissues. In this way, dermis plays an important role in repairing the skin and healing wounds (Kolarsick et al., 2011).

2.1.3. Hypodermis

Hypodermis or subcutaneous tissue is the lowermost layer of skin. This layer connects the skin with inner tissues such as fascia which is a coverage of muscles, muscle and bone. Subcutaneous tissue contains subcutaneous fat, blood vessels and nerves. The thickness contribution of the hypodermis to the soft tissue covering of the human body varies according to gender, age, nutritional status and living conditions within each regional body part. Its main function is to carry and connect tissues. It also acts as an energy store and mechanical protection and prevent the body from temperature fluctuations (Losquadro, 2017).

2.2. Wound and Wound Types

Wounds are the disruption or tear of anatomical structure of skin tissues that cause the skin to open or deform because of physical, chemical, mechanical and thermal damage due to cutting, penetrating or flammable factors. Wounds are classified according to the wound healing process and healing time. These are divided into two group as acute and chronic wounds.

2.2.1. Acute Wounds

Acute wounds are usually caused by trauma which occurs suddenly. The healing of these class of wounds are completed after an average of 8 to 12 weeks of healing. These wounds result from mechanical damage caused by cutting, puncturing, or tearing the skin tissue with hard objects. Besides mechanical damage, it can also be caused by irritation and exposure to extreme heat, radiation, electric shock, and corrosive chemicals. The care and healing time of these wounds depends on the severity of the wounds and the layer of skin in which the wound occurred. Cellular and molecular responses play a role in the healing of an acute wound. First of all, immune cells are directed to the area where the acute wound is located. Thanks to immune cells, the wound is cleared of pathogens. Fibroblast proliferation increases in that area. The wound bed is covered with oxygen and nutrients through new blood vessels which helps to healing (Martin & Nunan, 2015).

2.2.2. Chronic Wounds

Chronic wounds heal slower than acute wounds. The healing process can take more than 12 weeks and recurrence of these type of wound is common. These wounds are seen as the result of specific diseases. These diseases are known as diabetes, leg ulcers, tumors or serious physiological contaminations (El Ashram et al., 2021 ; Ghomi et al., 2019).

2.3. Wound Healing

The wound healing process is a continuous process that requires a suitable environment for wound healing and is affected by many factors. These factors can be listed locally and systematically. Local factors include radiation, hypothermia, infection, tissue oxygen tension, and pain that directly affect the wound. Systematic factors, on the other hand, are related to the health status of the person that directly affects the wound healing performance. The wound healing process includes the 4 healing phases of hemostasis and inflammation, migration phase, new tissue formation (proliferation) and remodeling (Ghomi et al., 2019).

2.3.1. Wound Healing Stages

Wound healing consists of four continuous stages as shown in Figure 2. 2. The first stage of healing, hemostasis, and inflammation is the stage that begins after the skin tissue is damaged. Fibrinogen is one of the main components of the connective tissues of the skin which provides coagulation of platelets and cells without blood called as exudates. With the formation of the fibrin network, the wound begins to coagulate, and coagulation is completed after a while. The inflammatory phase begins simultaneously with the hemostasis phase and usually lasts more than 24 hours. During this process, neutrophils in the blood and then phagocytes enter the wound environment and diffuse into the dead cells. In the migration phase the epithelial cells which are known as new and living cells, move towards the damaged area of the skin in order to replace the dead cells.

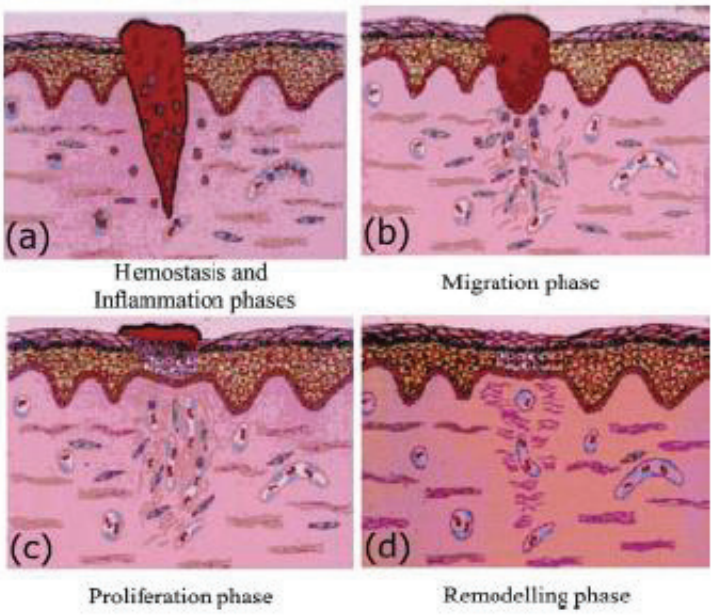

Figure 2. 2. Schematic representation of 4 wound healing stages.
(Source: Ghomi et al., 2019)

In the third stage called as the proliferation stage, the wound area is completely covered with epithelial tissue. During this phase new stroma, i.e., granulation tissues and new extracellular matrix of skin are formed. Microphages, fibroblasts, and blood vessels are formed a one structure together in the wound area. During this phase, which lasts about 2 weeks, the inflammatory phase gradually ends. The last stage of wound healing is the tissue remodeling stage which is also known as maturation phase. Fibroblasts help to completely close the wound surface by forming a new layer of skin (Ghomi et al., 2019).

2.4 .Wound Dressing Applications

Wound healing process is a biological process that is directly related to physiological parameters. While choosing the appropriate wound dressing for a specific wound type requires extensive knowledge about wound types, healing process and dressing applications. Thanks to the developments in science and technology, new wound dressings are being developed according to wound types. The correct selection of the dressing to be applied or developed is very important to ensure rapid and proper wound healing (Ghomi et al., 2019).

2.4.1. Property Requirements of Wound Dressing Applications

From past to today there have been lots of wound dressings improved according to the human skin needs. Since the healing of chronic wounds take longer time, wound dressings should shorten this process. Today, ideal wound dressings have some required properties to provide rapid and effective healing which are shown in Figure 2.3. An ideal wound dressing should provide a suitable environment on the wound surface and control the humidity around the wound by allowing gas exchange. It should eliminate the wound leaks by absorbing them. Ideal wound dressings have a key characteristic of collect excess exudate of wound while maintaining moisture at the wound bed (Boateng et al., 2008). While protecting the wound against external mechanical effects, it should also provide bacterial protection against microorganisms that may occur. By addition of antimicrobial agents, antibiotics or extracts to wound dressings antibacterial activity can be achieved. It should reduce necrosis on the wound surface. It should be easily changed and removed without sticking to the wound and causing trauma which can be provided by keeping moist the wound area. In addition to the desired properties, it should be biodegradable and biocompatible, non-toxic, and non-allergenic. Also, dressing should reduce the pain of the wound. Lastly, the cost of wound dressing must be acceptable (Ghomi et al., 2019).

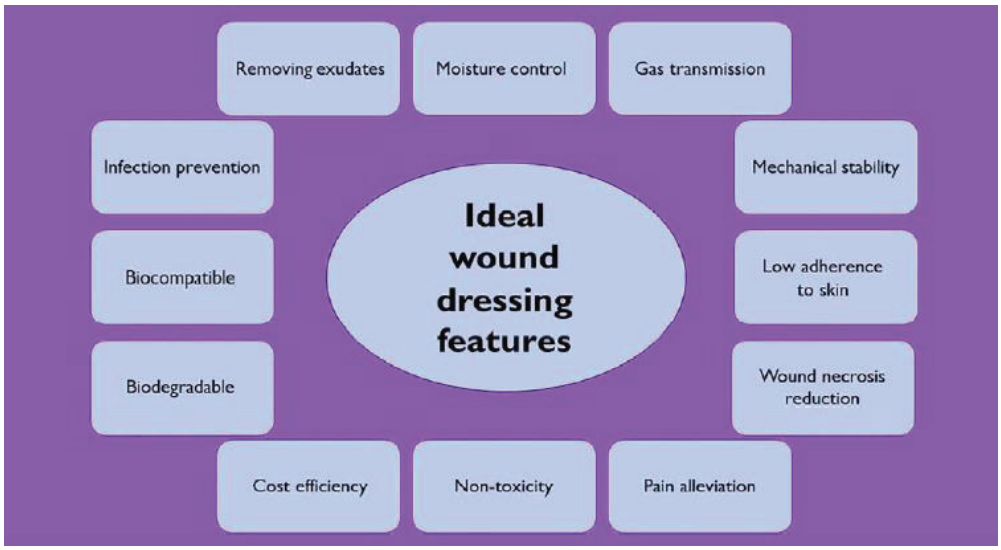

Figure 2. 3. Ideal wound dressing properties

(Source: Ghomi et al., 2019)

2.4.2. Traditional Wound Dressings

Many years ago, people used different materials such as flax, honey, animal fats and vegetable fibers as wound dressings for wound healing. Traditional dressings are also known as inert dressings. These dressings are the most widely used dressings as they are low cost and require a simple manufacturing process (Moore & Webster, 2018). Generally traditional dressings consist of gauze, cotton pads, lint, and bandages made of synthetic or natural materials. The purpose of using these traditional dressings is to absorb the wound exudate and protect the wound from contamination. Since these dressings are dry, they cannot provide the necessary moist environment for wound healing. In addition, due to leakage from the wound, these dressings become moist and adhere to the wound. For this reason, they cause trauma to the wound while being removed. They need to be changed frequently to avoid maceration of healthy tissues. Their cost is low, but they do not offer a quick and effective solution for wound healing. Since they cannot provide the necessary moist environment to the wound and cause trauma to the wound during replacement, more advanced modern wound dressings are used, which provide a more humid environment for the wound (Dhivya et al., 2015).

2.4.3. Modern Wound Dressings

Modern dressings have been developed to provide a more favorable environment for wound healing, rather than simply covering the wound and absorbing the leakage as with traditional dressings. Modern dressings are biodegradable and biocompatible compared to traditional dressings. They provide a moist environment to protect the wound from dehydration and were developed to accelerate healing. These advantages of modern dressings compared to traditional dressings lead to relieve pain and help to heal wound environment (Moore & Webster, 2018). There is a wide variety of modern dressings available on the market, depending on the type of wound and the cause of its formation. Modern dressings classified as passive interactive and bioactive dressings. Nowadays, the commonly used modern dressing types are interactive and bioactive dressings since passive dressings are not provide moist environment and permeability of gas exchange. The dressings known as semi-occlusive or occlusive, available in film, foam, hydrogel, and hydrocolloid forms, belong to the class of interactive dressings. These dressings are

seen as a barrier against the entry of bacteria into the wound environment. Bioactive dressings, which are another important modern type of wound dressing, contain bioactive agents for wound healing (Dhivya et al., 2015 ; C. Shi et al., 2020).

2.4.4. Hydrogel Wound Dressings

Hydrogels are hydrophilic materials, and their structure is three-dimensional. They can be produced by freeze drying method and particulate leaching method. Hydrogels are insoluble in water, and their water absorption properties are very good. They can absorb water from approximately 10% to thousands of times their weight. Thanks to their perfect moisturizing abilities, hydrogels keep the wound moist and play an important role in clearing necrotic tissue. Additionally, because hydrogels are transparent materials, a wound can be monitored without removing with a hydrogel-coated dressing (Shi et al., 2020). Hydrogel dressings do not require a secondary dressing. Thanks to its flexibility, it can be cut to fit around the wound (Boateng et al., 2008). The disadvantages of hydrogels include low barrier property and low mechanical strength. The low barrier property may cause the growth of bacteria producing bad odor in wounds due to accumulation of wound exudate. A second layer is required to improve this barrier property. Low mechanical strength makes the material difficult to process (Dhivya et al., 2015 ; Shi et al., 2020).

2.4.5. Hydrocolloid Wound Dressings

Hydrocolloid dressings are 2-layer interactive dressings, an inner colloid layer, and an outer waterproof colloid layer. These interactive dressings are made from gel-forming carboxymethylcellulose, gelatin and pectin elastomeric agents. Unlike hydrogels, hydrocolloids have barrier property against bacteria and are permeable to water vapor. These hydrocolloids form gels when in contact with wound exudate and provide a moist environment around wound which protect granulation tissue by absorbing and holding the exudates. They are not suitable for use on wounds with high exudates, so they are preferred as secondary dressings (Boateng et al., 2008 ; Dhivya et al., 2015).

2.4.6. Semi Permeable Films

Semi permeable film dressings have been used for a long time which are produced by solvent casting method. Semi-permeable films are wound dressings that are permeable to water vapor oxygen and carbon dioxide. They act as a barrier against the passage of bacteria. Since they are transparent, wound healing can be monitored without removing the dressing. These dressings are made of transparent and adhesive polyurethane material. Film dressings have limited wound exudate absorption capacity, so they are not suitable for wounds with high excessive exudate. Therefore, modern semi-permeable film dressings are recommended for the healing of epithelialized wounds, superficial wounds and shallow wounds with low exudates (Thomas et al., 1988 ; Debra & Cheri, 1998).

2.4.7. Semi Permeable Foams

Semi-permeable foam dressings are made from hydrophilic and hydrophobic foam using the freeze-drying method. Foam dressings provides gas and water vapor gas passage thanks to its porous structure and thanks to its hydrophobic outer layer, they protect wound from external fluids. The foams have a variety of absorbing excess exudates of wounds according to the thickness. Generally, they are preferred to use as primary dressings due to their high absorption and permeability characteristics. Therefore, these dressings play a major role in the healing of wounds with high exudates but are not recommended for wounds with low exudate or dryness. The disadvantage of these wound dressings is that they are used in very leaky wounds and therefore need to be changed frequently even though they have a high absorption capacity (Dhivya et al., 2015 ; Ramos-e-Silva & de Castro, 2002).

2.4.8. Nanofiber Wound Dressings

Electrohydrodynamic (EHD) technique is a material production method that is formed by spraying a polymer solution in the form of a fine jet with the effect of the electric field. This method allows to produce materials in two different morphologies, namely electrospinning and electrospraying which provides formation of nanofibers and nanoparticles respectively. The main difference of electrospinning and electrospraying

method is viscosity of polymer solution. If the polymer solution has low viscosity, then nanoparticles can be obtained. Otherwise, if the polymer solution has a viscous property, nanofibers can be produced by electrospinning method. EHD is a low-cost, time-efficient, multi-functional method, but it is also used to turn pharmaceutically relevant agents into polymer carriers (Zare et al., 2011).

With the developments in nanotechnology, nanofiber wound dressings have become one of the prominent applications for biomedical applications because nanofiber dressings can mimic the fibrous structure of extracellular matrix of skin (ECM). Due to this mimicry ability, the attachment, growth, and migration of fibroblasts is promoted and as a result, skin tissue in the wound area is regenerated (Memic et al., 2019). Electrospinning method has many advantages such as providing large surface area and aspect ratio and porosity, encapsulating multiple drugs, absorbing wound exudates effectively, providing protection against bacterial infections, allowing gas permeability, and affecting cell proliferation (Kimna et al., 2018 ; Rad et al., 2018 ; Zahedi et al., 2010). Electrospinning is an efficient and beneficial technique to produce continuous fiber from polymer solution with electric field. The mechanism of the electrospinning process consists of the basic electrospinning assembly, a reservoir with the solution (typically a syringe), a high-voltage power supply, a pump, and a metal collector as can be seen in Figure 2. 4. At the beginning of the electrospinning process, the polymer is extruded towards the needle tip with the help of the syringe pump, and the polymer solution is observed as a droplet at the needle tip. After to the electric field is formed between the needle tip and the collector, the droplet at the needle tip transforms from a hemispherical shape to a conical shape which is called as 'Tylor Cone'. With the increase of the electric field, more electric charge accumulates on the droplet. This increased electric field deactivates the surface tension of the polymer droplet, which allows the polymer solution to be jetted from the needle tip to the collector. The solvent evaporates as the polymer jet is ejected from the needle tip. As a result, fine fibers with random orientation with nano size are collected in the collector (Quek et al., 2019).

The morphology and mechanical properties of electrospun materials are directly related to the flow rate of the polymer solution, the applied voltage, the distance between the needle tip and the collector, the viscosity of the polymer solution and environmental conditions (Memic et al., 2019).

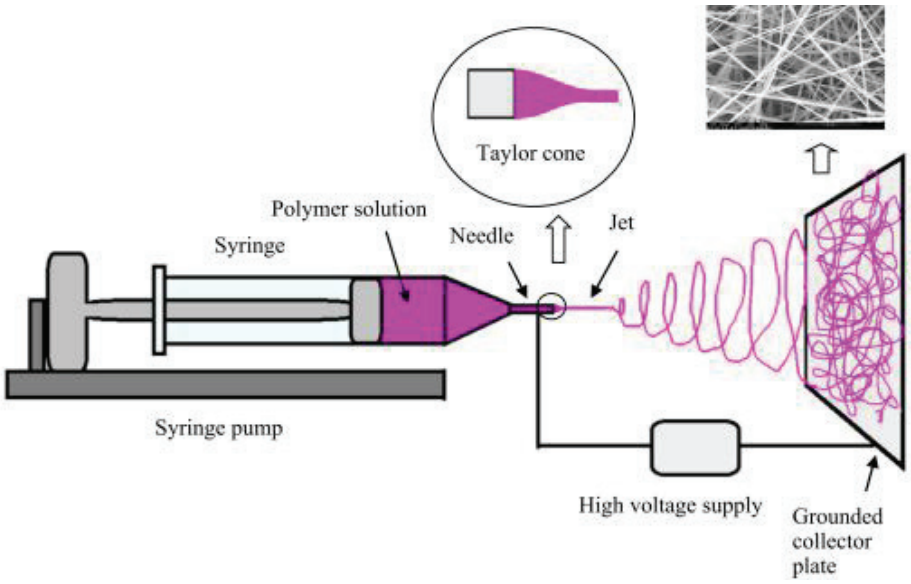

Figure 2. 4. Illustration of electrospinning system.

(Source: Quek et al., 2019)

Considering all these features of the electrospinning method, this method has a great importance especially for drug delivery, encapsulation, and tissue engineering applications.

2.4.9. Bioactive Wound Dressings

Bioactive dressings are the most advanced type of modern dressings which are derived from biomaterials used in wound healing applications. They can be also called as biological dressings. These wound dressings have lots of unique characteristics. They are biodegradable, biocompatible with tissues and have non-toxic property and they are containing natural extracellular matrix components (Ueno et al., 1999). The biomaterials used for these dressings have the advantage of being able to mimic the natural tissue matrix of the skin and even form a part of it. They provide new tissue formation from wound side (Boateng et al., 2008). They can be obtained from both natural, chitosan, collagen, alginate, zein and synthetic resources. To obtain bioactive dressings sometimes polymers can be used in combination with the addition of antimicrobials to improve the wound healing process. Thanks to these developments, bioactive wound dressings are the most effective dressings when compared to other dressing types (Dhivya et al., 2015).

2.4.10. Polymeric Drug Delivery Dressings

Modern wound dressings consist of biomaterials which are derived from natural or synthetic resources can contain antimicrobial agents, essential oils or drugs. To achieve effective and quick wound healing polymer-drug complexes can be used depending on wound type. Bioactive dressings containing antibiotics provide tissue compatibility, prevent bacterial formation with antimicrobial effect and require less intervention. Polymer dressings containing drugs help to reduce the risk of systemic toxicity by providing dose adjustment and controlled release of antibiotics. It is ensured that the drugs are released to the wound area in a consistent and continuous manner over a long period of time. Modern drug-loaded dressings developed for wound healing in the form of films, foams, gels. Nanofibers, porous sponges, or polymeric scaffolds can also be used in development of multifunctional wound dressing materials (Boateng et al., 2008).

2.5. Polymers Used in Wound Dressing Applications

Modern wound dressings are classified into two groups as synthetic and natural polymers. Natural or synthetic polymers can be used for wound healing applications. As synthetic polymers, polyvinyl alcohol (PVA), polylactic acid (PLA), polycaprolactone (PCL) are the polymers commonly used in wound dressings. However, synthetic polymers are not as biocompatible with the body as natural polymers. They are not biodegradable and do not have the ability to mimic skin tissues and provide cell growth and immune response. For this reason, the preference of wound dressings synthesized from natural polymers rather than synthetic dressings provides a faster and more effective solution to wound healing by providing tissue compatibility without creating toxic effects. For this reason, natural polymers, or biopolymers such as gelatin, , collagen, chitosan, zein have the great interest due to their biocompatibility with human tissues, environmental friendliness, and no toxic effects (Kurtoğlu & Karataş, 2009).

2.5.1. Gelatin

Gelatin is one type of protein which is derived from native collagen by controlled hydrolysis (Deshmukh et al., 2017). Gelatin biopolymers have been extensively studied

in the literature due to their biodegradability and their potential for commercial use. Gelatin is a biopolymer with biocompatibility and hemostatic properties. It also has reduced cytotoxicity, low antigenicity and aids cellular growth and attachment. However, its poor mechanical properties oblige it to be used in combination with other polymers. In addition to these wound dressings of gelatin with antimicrobial agents provide in vitro and in vivo antimicrobial activity since gelatin has no antimicrobial activity on its own. Also, the fast degradation time and highly hydrophilic surface of gelatin make it unsuitable to use without other polymers. Zheng et al. prepared hydrogels by incorporated tannic acid into gelatin blended with gellan, which is a polysaccaride, for antibacterial wound dressing for full thickness wounds. They observed excellent antimicrobial activity against S. aureus, E. coli, and drug-resistant bacteria by using disk diffusion method (Zheng et al., 2018). Shi et al. fabricated gelatin-based elastomer nanocomposite membrane with ciprofloxacin and polymyxin B sulfate loaded halloysite nanotubes (HNTs). They observed increase of hnts good mechanical properties achieved and gelatin-based nanocomposite showed antimicrobial activity against gram negative and positive bacteria (Shi et al., 2018). Therefore, gelatin-based dressings are suitable for the treatment of infected, exuding and bleeding wounds (Ndlovu et al., 2021).

2.5.2. Collagen

Collagen is a protein which is an important component of connective tissue and found in human body. In the wound healing process, collagen plays a very active role in all stages from the beginning of healing to the final scar tissue formation. Collagen acts as a stimulant for fibroblast formation and accelerates endothelial cells reaching the injured tissue which helps to accelerates wound healing process (Babu, 2000). Also, collagen matrices can collect wound exudates and wound waste. There are lots of studies in literature related with collagen. In the study of Adhiran and coworkers, microspheres incorporated collagen membranes was used to reduce both bacterial growth and MMPs, (metalloproteases), activity which is a group of proteolytic enzymes increased in chronic wounds (Adhirajan et al., 2009).

2.5.3. Chitosan

Chitosan is a natural linear polysaccharide obtained from chitin which is found in the shells of crustaceans. Structure of chitosan, linear polysaccharide, represented in Figure 2. 5 which is composed of randomly distributed β-(1-4)-linked D-glucosamine (deacetylated unit) and N-acetyl-D-glucosamine (acetylated unit). Chitosan is biocompatible, hydrophilic, and degradable biopolymer therefore it is very well suited for the human body applications. It does not show toxic properties, on the contrary, it has antimicrobial properties. It is known that chitosan accelerates the formation of granulation tissue in the proliferation stage, which is one of the wound healing stages (Kurtoğlu & Karataş, 2009). Also, chitosan biofunctionality can be improved by addition of antimicrobial or bioactive agents such as drugs, silver, zinc, vitamins and anti-inflammatory agents (Miguel et al., 2019). Since chitosan has variety of advantages and properties, it can be suitable for wound dressing applications. However, chitosan has also low mechanical properties and thermal stability. Therefore, it can be used with other polymers to make their mechanical properties improved. There are few studied listed in table 1 related with chitosan. Morgado and coworkers, fabricated polyvinyl alcohol (PVA)/Chitosan asymmetric membranes for wound dressing by supercritical carbon dioxide ($scCO_2$)-assisted phase inversion method. They found that the membranes showed high antibacterial activity against *E.coli*. Combination of chitosan with PVA improved the mechanical properties and stability of the membranes (Margado et al., 2014). In another study, Tamburaci and Tihminlioglu prepared chitosan membranes incorporated with Polyhedral oligomeric silsesquioxanes (POSS) with solvent casting technique to improve mechanical properties. Also chitosan/POSS composite membranes did not show any toxic effects and cell proliferation was achieved (Tamburaci & Tihminlioglu, 2018 ; Miguel et al., 2019). Tamburaci et al., fabricated chitosan (CS) and OctaTMA-POSS nanocomposite membrane for bone tissue regeneration obtained by freeze-dry method. It was found that, incorporation of chitosan-POSS enhanced cell proliferation and modulus of scaffold (Tamburaci & Tihminlioglu, 2018). Jayakumar et al., studied ZnO incorporated chitosan sponges for wound healing. Antibacterial, blood coagulation, swelling, cytotoxicity and cell adhesion properties of chitosan sponges were analyzed. As a result, they found that chitosan sponges containing ZnO had enhanced swelling, blood clotting, and antibacterial activity. Cytotoxicity results showed that the

material was non-toxic to human dermal fibroblast and Vero cell line. All these results proved that ZnO-chitosan nanocomposite sponge is preferable and potential wound dressing (Jayakumar et al., 2011). In another study, Anisha et al., developed chitosan with hyaluronic acid sponges which contains silver nanoparticles. The chitosan sponges showed antibacterial effect against gram negative and positive bacteria and cytotoxicity property was tested on human fibroblast cells. Addition of silver nanoparticles decreased the cytotoxicity and cell attachment was increased (Anisha et al., 2013). Ong et al., produced silver nanoparticle incorporated chitosan polyphosphate dressing to accelerate blood clotting and to provide antibacterial activity against wound pathogens of Pseudomonas aeruginosa and Staphylococcus aureus. The hemostatic efficacies of dressings were evaluated according to in vitro studies. As a result, addition of silver nanoparticles was effective in reducing mortality compared to standard gauze treatment in a full-thickness wound model contaminated with high levels of P. aeruginosa (Ong et al., 2008).

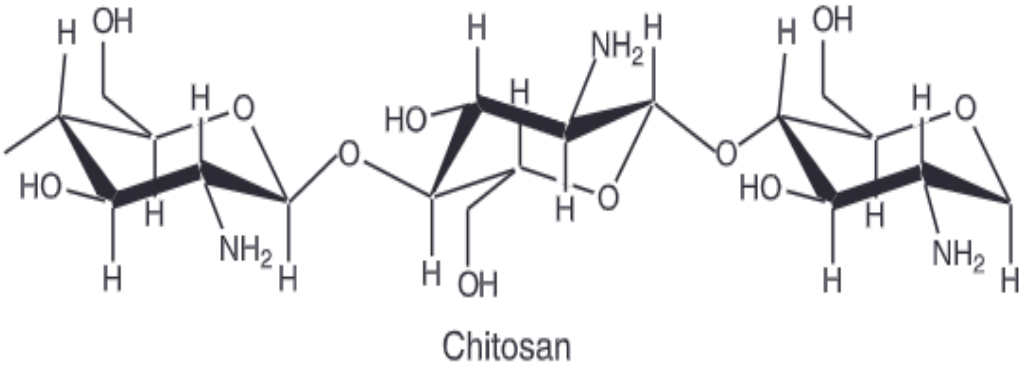

Figure 2. 5. Structure of chitosan
(Source: Nilsen-Nygaard et al., 2015)

Table 2. 1. Chitosan based wound dressings and tissue regeneration studies

Method	Purpose	References
Membrane	Wound dressing	(Morgado et al., 2014)
Film	Bone tissue regeneration	(Tamburaci & Tihminlioglu, 2018)
Scaffold	Bone tissue regeneration	(Tamburaci & Tihminlioglu, 2018)
Sponge	Wound dressing	(Jayakumar et al., 2011)
Sponge	Wound dressing	(Anisha et al., 2013)
Gel like PECs (polyelectrolyte complexes)	Wound dressing	(Ong et al., 2008)

Film dressings are mostly used for superficial and low exuding wounds. It allows gas passage and protects the wound from bacteria. However, sponge-like wound dressings allow gas permeability more than film dressings due to their porous structure and are preferred for wounds with dense wound exudates since they have high swelling percentages (Boateng et al., 2008). In this thesis, chitosan sponge was used as bottom layer to provide mechanical strength, gas transmission and collect exudates around wound.

2.5.4. Zein

Zein is a natural protein-based polymer which is a storage corn protein and obtained from renewable resources (Figure 2.6, 2.7). This completely biocompatible, biodegradable polymer is environmentally friendly. In the last few years, zein has been studied for polymer application as a possible ‘green’ raw material. It is a transparent, odorless, tasteless, edible polymer and is therefore used in processed foods and pharmaceuticals. Zein has three major fractions named α-, β-, and γ-zein. The α -zein is

the major fraction of zein which contains 75–85% of the whole zein in corn while β-, and γ-zein constitute only 10-15% and 5-10% of zein in corn, respectively. The α -zein shows higher solubility character than other two fractions of it and it is soluble in approximately 50 to 95% alcohol without needed any reducing agents or any buffers. Therefore, α-zein is the main type zein commercially available in the market which was represented in Figure 2.8 (Luo & Wang, 2014). Zein which is generally recognize as safe biomaterial (GRAS) consist of helical wheel conformation that consist of nine homologous repeating units as inner part, and they are hydrophobic. Upper and lower surface are connected by glutamine bridges which stabilized nine repeating units by hydrogen bonds, and they are hydrophilic that are shown in Figure 2. 8 and Figure 2.9 (Luo & Wang, 2014). Zein can also be used in several application areas such as textile, cosmetics, adhesives, and biomaterials (Kimna et al., 2018).

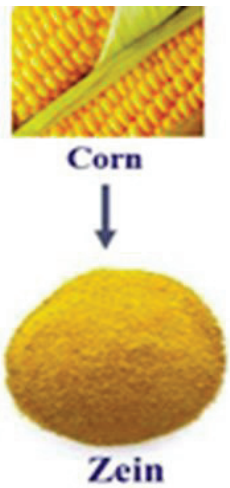

Figure 2. 6. Representation of Zein

(Source: Bharathi et al., 2019)

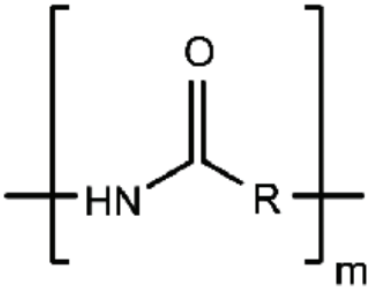

Figure 2. 7. Chemical representation of zein

(Source: Bharathi et al., 2019)

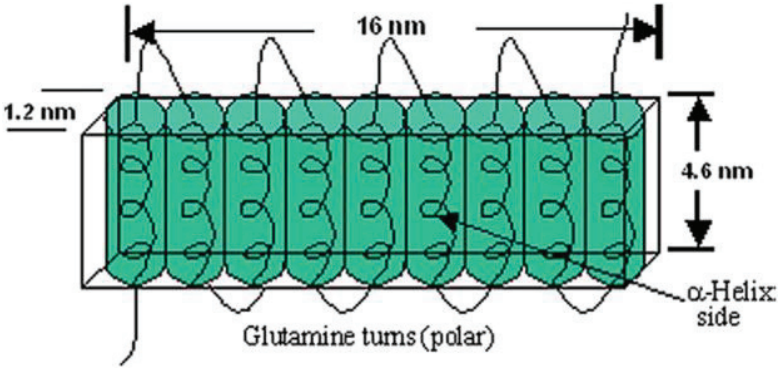

Figure 2. 8. Structure of zein

(Source: Luo & Wang, 2014)

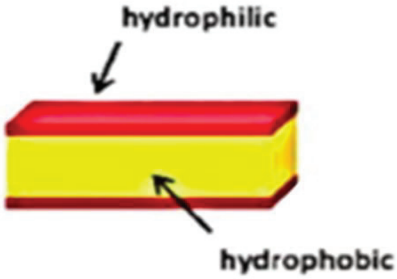

Figure 2. 9. Representation of Zein's hydrophilic and hydrophobic parts.

(Source: Luo & Wang, 2014)

Zein is an amphiphilic protein which is a property depending on processing method. Due to processing method materials can be both hydrophobic and hydrophilic. Commercially available zein is insoluble in water, but soluble in alcohol, due to its non-polar amino acids. However, the insolubility in water makes zein selective polymer for oral and dermal applications. Also, this property of zein provides ease of use for controlled oral drug delivery matrix applications (Georget et al., 2008). Beside this solubility character, zein can be easily fabricated in the form of films, microspheres, nanoparticles, micelles, gels, foams, and fibers (Kimna et al., 2018).

Zein has been used for numerous applications like drug delivery and tissue engineering areas. Few studies exist in literature related to zein nanofibers for wound dressing applications which were listed in Table 2. 2 Zein/cellulose acetate hybrid nanofiber scaffolds were fabricated by Ali et al. The addition of cellulose acetate (CA) provided good mechanical and wetting properties. They observed that the addition of CA decreases the nanofiber diameter. CA also improved the thermal stability of pristine zein

nanofibers. As a result, it was suggested that the developed scaffold can be used for tissue engineering and other biomedical materials (Ali et al., 2014). Beside pure zein nanofibers without antibacterial agent, essential oil based-zein nanofibers for antimicrobial effect were also studied. Lui end coworkers have developed zein thyme oil (TEO) nanofiber membranes for wound healing applications by using electrospinning process. According to their study, with the addition of thyme oil to zein fiber antimicrobial activity was achieved against *E.Coli*. Also, in situ wound healing was analyzed in mice and it was observed that the fibrous membrane promotes wound healing for 11 days (Liu et al., 2019). In another study of Lin et al., they aimed to produce co-electrospun of zein-collagen nanofibers containing berberine drug, which was extracted from berberis and other plants, for wound healing. It was observed that zein increases the electrospinnability of collagen and with the addition of berberine extract, antibacterial activity was provided (Lin et al., 2012). To impart antimicrobial activity into zein nanofibers, in literature, nanoparticles are generally incorporated into zein nanofiber mats. Dashdorj et al., added silver nanoparticles into zein nanofibrous mats. They found that Ag nanoparticles provided antimicrobial effect against both gram positive and negative bacteria. Besides that, cell viability, good cytocompatibility were observed in fibroblast cells (Dashdorj et al., 2015). Ghorbani et al., fabricated Zein/Polycaprolactone/Collagen nanofibers incorporated with Zinc oxide (ZnO) nanoparticles and aleo-vera is used as therapeutic agent to enhance the collagen sytnthesis. They observed that the collogen electrospinnability was improved with the addition of zein. Mechanical strength of zein was improved by the addition of PCL and the incorporation of ZnO and Aleo-vera enhanced the tensile strength further. Additionally, antibiotic added zein nanofiber wound dressings were developed in literature. Kimna et al., fabricated bilayer zein membranes composed of incorporated zein electrospun nanofibers as bottom layer and zein film containing glycerol plasticizer as upper layer.As a result, the developed membrane provides good mechanical property, antimicrobial activity, and non-toxic behavior (Kimna et al., 2019). In order to improve mechanical properties of zein, clay additives were also used in literature. Gunes et al., fabricated bilayer wound dressing consist of zein/montmorillonite (MMT) film and Zein/MMT nanofibers. As an upper layer zein/MMT film was used which includes H. Perforatum oil which has a wound-healing effect by inducing fibroblast migration and bottom layer contains Zein/MMT nanofiber. In the study of Gunes and coworkers, montmorillonite (MMT) a non-toxic nano-clay, was used in both production of zein films and nanofibers to enhance the zein's poor

mechanical and swelling properties. It was found that the developed wound dressing has suitable mechanical, thermal and antimicrobial properties (Ghorbani et al., 2020). Ciu et al., prepared poly (-vinyl alcohol)-stilbazol quaternized (PVA-SbQ)-zein co-electrospun nanofibers incorporated with vaccarin drug. They used PVA-Sbq as crosslinking agent to enhance mechanical properties and surface wettability of zein (Cui et al., 2015).

Table 2. 2. Zein based studies

Method	**Purpose**	**References**
Scaffold	Tissue engineering	(Ali et al., 2014)
Nanofiber	Wound dressing with Essential oil	(Liu et al., 2019)
Nanofiber	Wound dressing with Berberine extract	(Lin et al., 2012)
Nanofiber	Wound Dressing with Ag (silver) additive	(Dashdorj et al., 2015)
Nanofiber	Wound Dressing with ZnO (zinc oxide) additive	(Ghorbani et al., 2020)
Membrane	Wound Dressing with Gentamycin drug	(Kimna et al., 2019)
Nanofiber & Film	Wound Dressing with MMT clay additive	(Gunes et al., 2020)
Nanofiber	Crosslinked Wound Dressing with Vaccarin drug	(Cui et al., 2015)

Despite the advantageous aspects of zein, its mechanical strength is low. Unfortunately, the presence of crosslinking agents can lead to toxic side effects. In addition, undesirable reactions between drugs or extracts and cross-linkers may lead to the formation of toxic or inactive species (Liu et al., 2005). Therefore, combination of zein with the antimicrobial agent encapsulated halloysite clay nanotubes may allow to generate novel green materials with enhanced mechanical properties and a sustained release of antimicrobial agent. Since there are few studies exist related to zein nanofiber for tissue engineering applications, in this thesis, zein -antibiotic loaded halloysite nanofiber mats will be prepared as the upper layer of wound dressing in order to obtain a sustained release of antibiotic.

2.6 . Importance of Halloysite Nanotubes for Development of Functional Nanocomposites

Halloysite Nanotubes (HNTs) are green, not hazardous materials which are cheap, and available in market. Halloysite clay is a naturally formed material which has a tubular formation composed of alumina-silicate sheets rolled into tubes with a chemical formula of $Al_2Si_2O_5(OH)_4$. These nanotubes have unique chemical, physical properties. HNTs have approximately 1000 nm length, about 50-80 nm diameter and 10-15nm internal lumen. The structure of HNTs was shown in Figure 2. 10 (de Oliveira & Beatrice, 2018). Inside of nanotubes composed of Aluminol groups (Al-OH) while outside of tubes contain Siloxane groups (Si-O-Si). Inner charge is positive containing AL-OH, however, outer charge is negative containing Si-O-Si groups. This charge difference makes HNTs favorable reinforcement because, different drugs or antimicrobial agents can be adsorbed or loaded whether they have positive or negative surface charge. HNT show different surface charge depending on pH.

Halloysite, a biocompatible "green" material, is a preferred reinforcement due to its simple processing and low cost, and an innovative additive for polymer composites. Halloysite clay minerals are added as inorganic reinforcement materials for polymers. The nano-sized lumens of these tubes provide a very suitable environment for loading bioactive molecules. These bioactive molecules include self-healing, anti-corrosion, antimicrobial agents, proteins, DNA, drug or antibiotics.

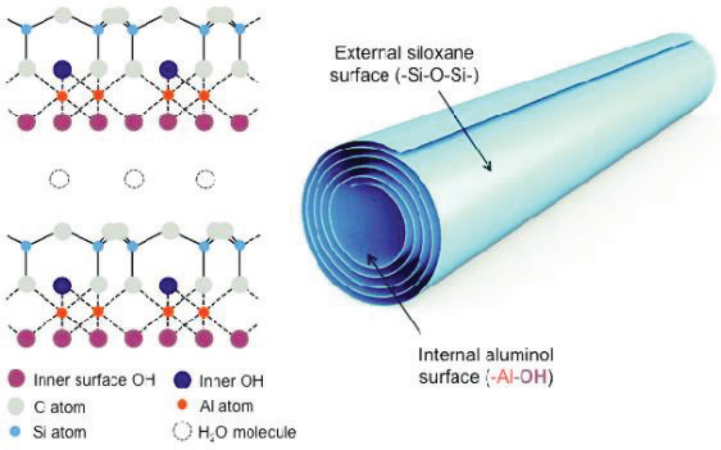

Figure 2. 10. Structure of Halloysite nanotube (HNT)
(Source: de Oliveira & Beatrice, 2018)

HNTs, which are used as additives in polymers, can improve mechanical, thermal and wettability properties. HNT is also known as nontoxic and biocompatible material which has been proven in different cells and tissues. Therefore, it can be used for various biomedical application due to easily incorporation of drugs into tubes.

Table 2.3, tabulates the studies done by using HNTs in wound dressing applications. Pavliňáková et al., produced Polycaprolactone-Gelatin nanofibers reinforced with 3 different HNTs with different ratios as 0.5, 1.0, 3.0, 6.0, and 9.0 wt%. Addition of HNTs improves the mechanical properties of nanofiber wound dressing. Beside, they achieved non-cytotoxic behavior on the interaction with mouse fibroblasts NIH-3T3 cells (Pavliňáková et al., 2018). Shi et al., fabricated gelatin-based elastomer incorporated with ciprofloxacin and polymyxin B sulfate loaded HNTs with different ratios (0%, 5%, 10%, 15% and 20 wt%). They obtained longer drug release from the dressing. In addition, the enhanced mechanical properties and thermal stability were achieved with the addition of HNTs (Shi et al., 2018). Besides of these wound healing applications, Gorrasi and coworkers prepared zein-HNTs composite films as food packaging film. HNTs are encapsulated with potassium sorbate (KS) which is a commonly used preservative for food packaging. They found that HNTs enhance thermal and mechanical properties of the films and provided sustained release of the drug form the food packaging film (Gorrasi & Vertuccio, 2016).

Table 2. 3. Halloysite nanotube studies

Method	**Purpose**	**Reference**
Nanocomposite membrane	Wound dressing	(Shi et al., 2018)
Nanofiber	Wound dressing	(Pavlináková et al., 2018)
Film	Food Packaging material	(Gorrasi & Vertuccio, 2016)

CHAPTER 3

MATERIALS AND METHOD

3.1. Materials

Zein from maize (MW: 40 kDa, Sigma-Aldrich), was used for nanofiber formation. Ethanol (≥99.5%, Sigma-Aldrich) was used as a solvent to prepare zein solution. Halloysite nanotube (HNT) (Sigma-Aldrich) was used as a nano reservoir to encapsulate Vancomycin drug (Koçak Farma). Low molecular weight chitosan (Sigma-Aldrich) was used to produce the porous sponge layer as lower layer. Acetic acid was purchased from Merck and used as a solvent for the preparation of the chitosan solution. Phosphate buffered saline (PBS) tablets (Invitrogen, Thermofisher Scientific) were used for in vitro drug release, zeta potential measurement, and swelling studies.

3.2. Preparation of Upper layer

3.2.1. Preparation of Vancomycin Loading into HNT (Halloysite Nanotube) by Vacuum Method

Firstly, 1mg/ml vancomycin drug dispersion was prepared in DI water. After that different amount of Vancomycin: HNTs (1:1, 1:2, 1:5, 2:1 w t%) ratios were added to dispersion which was mixed for 30 min. Then, both ultrasonication and microfludization processes were applied separately to provide homogeneous dispersion as well as to increase the encapsulation efficiency of HNT.Ultrasonication was proceed for 15 minutes at 15 amplitude and repeated three times. Microfludization process was carried out as three passes at 10,000 Psi pressure. After applying sonication and microfludization, vacuum oven (MMERT) was used to provide encapsulation of drugs into HNTs. The dispersions taken out from the vacuum oven were mixed by magnetic stirrer initially for 15 minutes and then put back into the vacuum oven for 20 minutes. This procedure was repeated 3 times. After that, dispersions were put into centrifuge at 4000 rpm for 10-minutes. Centrifuged samples were separated as solid and liquid parts, and remaining

liquid samples were analyzed by UV spectrophotometer at 280 nm where the drug has a maximum peak. Concentration of drug in the remaining solution was calculated in order to find the loading and encapsulation efficiencies were measured. Centrifuged solid samples were then dried in the oven at 50°C for 24 hours.

3.2.2. Preparation of HNT-Zein Fibers by Electrospinning Method

Zein (25 wt/v %) was dissolved in 70 v/v % of ethanol solution. Different concentration of HNTs (1,3 and 5 wt%) were added into zein solution which were mixed for 1 hour. After that 4ml of zein solution which contains 1 to 5 wt% of HNTs was taken with needle and electrospun by using different flow rates as 1,2 3, 5, 7 and 10 ml/h syringe pump, 20kV power source. The distance between needle (diameter of 21 G) and collector is 10cm. The single layer electrospun wound dressings were put into desiccator for further characterization tests after electrospinning was completed.

3.2.3. Preparation of Vancomycin Loaded HNT – Zein Fibers by Electrospinning Method

25 wt/v % zein was dissolved in 70 v/v % ethanol solution by using magnetic stirrer for 3 hours continuously. Then, different amount of drug loaded HNTs powders were dispersed in 70 w/v % ethanol solution and added into the zein solution. They are mixed for 1 hour. After the prepared 4ml of zein solution containing 1,3 and 5 wt/wt % of drug loaded HNTs was electrospun with 21G needle diameter at 20kV power source. The distance between needle tip and collector was kept constant as 10 cm and flow rate of 3 ml/h. The mono and bilayer electrospun wound dressings were put into desiccator for further characterization tests after electrospinning was completed.

3.3. Preparation of Chitosan Sponge

2 wt/v % of low molecular weight chitosan was dissolved into 2 v/v % acetic acid solution and continuously stirred for 4 hours. After chitosan was completely dissolved, solution was poured into petri dish then it was pre-frozen at -20°C refrigerator for 24h. Next, chitosan sponges were obtained by lypholization of the frozen samples in freeze

dryer, (Labconco, FreeZone 4.5 liter Freeze Dry Systems, 77500-77510 Series Models) for 48 hours at -46°C and, under 0,018 mbar vacuum. After that chitosan sponges were put into desiccator and stored for further tests.

3.4. Preparation of Bilayer Wound Dressing

Bilayer wound dressing was prepared by coating Zein-NHT electrospun nanofibers on top of the chitosan sponge layer by electrospinning method. Drug loaded and unloaded HNT incorporated Zein nanofibers were coated on the chitosan sponge. Zein-HNT electrospun nanofibers with two different thickness was coated on the chitosan sponge. At the end of this process, bilayer nanofiber-sponge wound dressings were prepared.

3.5 . Characterization of Mono and Bilayer Membranes

Mono and bilayer wound dressings were characterized according to their morphology, contact angle, zeta potential, encapsulation efficiency, thermal characteristics, mechanical strength, water uptake, *in vitro* degradation and, drug release studies and antibacterial activity.

3.5.1. Morphology

Morphology of single layer and bilayer wound dressing was analyzed by using SEM (Quanta FEG 250, 7x10-2 mbar and 15mA). Average fiber diameter of zein nanofibers as well as the thickness of bilayer and single layers were measured. Before SEM analysis, samples were covered with gold in the presence of Argon gas using Emitech K550X Spot Coater. To measure average fiber diameters, Image J program was used.

3.5.2. Fourier-Transformed Infrared Spectroscopy Analysis (FTIR)

ATR-FTIR (Shimadzu FTIR-8400 s) was used to analyze chemical composition of powder forms of pure zein fibers as well as different amount of HNT loaded zein fibers. Samples were investigated at the wavelength range from 4000 cm^{-1} to 400cm^{-1}. Interactions between zein, HNT and antibiotic drug was also evaluated by using FTIR.

3.5.3. Zeta Potential Analysis

Since the zeta potentials of HNT can affect the drug loading. Therefore, the zeta potantials should be measured at different pH values. Surface charges of neat HNT and drug loaded HNT were investigated by using Malvern Zetasizer Nano-Zs. Powders were dispersed in 1 x PBS at different pHs and at room temperature. pH was adjusted as 3, 5 and 8 by using 0.1M HCl and 0.1M NaOH. Powders were dispersed by using magnetic stirrer for 30 minutes and vortex for 5 minutes. The measurements were repeated three times to determine the average surface zeta potential value.

3.5.4. Encapsulation Efficiency

Vancomycin calibration curve (Figure A.1.) was drawn by using various vancomycin concentrations from 0 to 1 mg/ml vs absorbance values at 280 nm. While collecting remaining liquids after centrifugation, samples were put into UV spectrophotometer and absorbances were noted. With the help of the calibration curve, remaining sample's concentration was calculated. By subtracting initial concentration to remaining solution concentration, encapsulated drug concentration was found. Encapsulation efficiency (EE%) and loading efficiencies (LE%) were calculated by using the equations given below.

$$\text{EE\%} = \frac{\text{Total amount of drug} - \text{Amont of unbound drug}}{\text{Total amount of drug}} \text{ x } 100 \qquad \text{(Eqn 3.1)}$$

$$LE\% = \frac{\text{Total amount of drug} - \text{Amont of unbound drug}}{\text{Weight of nanoparticles}} \text{ x } 100 \qquad \text{(Eqn 3.2)}$$

3.5.5. Thermogravimetric Analysis (TGA)

Thermogravimetric analysis (TGA) was applied on Zein, HNTs, Vancomycin powders and, zein-HNT fibers by using Shimadzu TGA-51 Seteram thermogravimetric analyzer from room temperature to 750ºC, with a heating rate of 10 ºC/min under 20 mL/min N_2 atmosphere. Nearly 10 to 12 grams of each sample was used for analysis.

3.5.6. Contact Angle Measurement

Surface contact angle measurements was performed to determine surface wettability of each layer by using Attension Theta Optical Tensiometer. Contact angles were measured by dropping 5 µl. pure water on each layer. The average values of surface contact angles were reported in the thesis.

3.5.7. Open Porosity Measurement

Open porosity of monolayer chitosan sponge and bilayer chitosan sponge membrane (zein-3% HNT nanofiber coated chitosan sponge) were measured by using liquid displacement method. Samples were immersed into graduated cylinder which was filled with 10 ml of 99,99% pure ethanol (V_1). To replace air into the pores with ethanol, graduated cylinder was put into vacuum oven at 25˚C. After applying vacuum, total volume was measured as V_2. Samples were taken off from the graduated cylinder and residual solvent volume was noted as V_3. By using equation below, open porosity, ε% was calculated.

$$\varepsilon\% = \frac{(V1 - V3)}{(V2 - V3)} \text{ x } 100 \qquad \text{(Eqn 3.3)}$$

3.5.8. Mechanical Test

Mechanical properties of bilayer membranes were analyzed by using texture analyzer (TA XT Plus) with compression test according to the ASTM-D 5024-95a standard. Fiber coated and without fiber coated sponges had a 1cm height and 2cm diameters. Samples were compressed up to 75% of original height.

3.5.9. Water Vapor Transmission Rate

Water vapor transmission rate of one and bilayer wound dressings were analyzed by using operating system which consist of two chambers. The bottom chamber which was filled with constant amount (3ml) deionized water has a 100% relative humidity. The upper chamber has a probe which measures relative humidity % and temperature (C). The results can be read by using Datalogger SK-L 200 TH system. Mono and bilayer sponges had a diameter of 5cm placed in between two chambers. The WVP test was started when the relative humidity of probe reaches to 5% with the anhydrous CaSO4 column. After test was started, relative humidity % data was recorded in different time intervals. By using equation given below, WVP was calculated where L is thickness (cm), A is transfer area (m^2), t is time, R is the gas constant, V is the volume of the chamber. The slope of the equation is calculated using the graph with $[(P_{IL} - P_{1ui}) / (P_{IL} - P_{1ut})]$. P_{1L} and P_{1u} are partial pressure in the upper and lower chambers, respectively. The WVP and WVTR of mono and bilayer wound dressings were calculated as mol/min cm kPa and g / m^2 day respectively.

$$WVP = \frac{\text{Slope x L x V}}{\text{A x R x T}} \qquad \text{(Eqn 3.4)}$$

3.5.10. Swelling Ratio

Water uptake capacity or swelling ratio was calculated by immersing bilayer and monolayer dressings into 1 x PBS at pH=7.4 and 37 ° C. Firstly, dry samples were

weighted, and results were noted as Wd. The samples were incubated for 24 h and 48 h in 1xPBS simulated condition. Then, wet weight of the samples was measured as Ww. By using the formulation given below, swelling ratio was calculated.

$$\text{Swelling}\ (\%) = \frac{\text{Ww} - \text{Wd}}{\text{Wd}}\ \text{x}\ 100 \qquad \text{Eqn 3.5}$$

3.5.11. *In Vitro* Degradation Study

Enzymatic degradation of mono and bilayer dressings was analyzed by measuring weight loss. Samples were put into 1 x PBS at pH=7.4 by adding 1.5 mg/ml lysozyme to provide human blood environment. Also, sodium azide (0.01 wt. %) was added to prevent microbial contamination. Solution was changed every two days. Samples were collected on the 7th and 14th day weighted and noted as W_1. Dry samples were also measured as W_0. Weight loss percentages were calculated by using equation given below.

$$\text{Weight Loss}\ (\%) = \frac{\text{W0} - \text{W1}}{\text{W0}}\text{x}100 \qquad \text{(Eqn 3.6)}$$

3.5.12. *In Vitro* Drug Release Study

In vitro vancomycin drug release was performed under immersion in phosphate-buffered saline solution (PBS) while observing drug release from bilayer wound dressing consisting of electrospun drug loaded nanofibers coated on chitosan. Bilayer sponges were put into well plate. Before starting in vitro drug release firstly sponges were neutralized with 0.01M NaOH solution to prevent dissolution of the sponges in PBS. Afterwards samples were placed into 1 ml of 1x phosphate-buffered saline solution (PBS, pH=7.4). Drug release of samples were started in an orbital shaker (Thermoshake, Gerhardt) at 50 rpm with 37°C temperature. Drug release of vancomycin was determined by collecting samples at different time intervals. The media collected to measure drug

release was changed with fresh PBS solution to keep incubation volume constant. To calculate the cumulative drug release, the samples were analyzed on a UV-VIS spectroscopy (Varioskan) at 280 nm to determine the released Vancomycin as a function of time. Then, the experimental release data was used to determine the drug release kinetics. The rate of the drug release was fitted into the various mathematical release kinetic models explained below.

3.5.13. Determination of Kinetic Models

In drug release studies, semi-empirical and full-empirical experimental models are available to predict the drug release mechanism. In this study, Zero-order, First-order, Higuchi and Korsmeyer-Peppas release models were used to determine the vancomycin release kinetics from chitosan-zein/vancomycin loaded HNT bilayer dressing.

- *First Order Kinetic Model:* In the first order kinetic model, the main basis is drug concentration. The surface at which the drug is released, assumed as constant surface area during the spreading of drug. To calculate released drug amount, which is shown as M_t, equation defined below was used. K_1 is the first order rate constant, t is drug released time and M_0 is drug released amount at t=0. A semi-log plot of the cumulative percentage of residual drug versus time was plotted to evaluate the kinetic parameters of the first-order release model.

$$Mt = Mo\, e^{-K1t} \qquad \text{(Eqn 3.7)}$$

- *Higuchi Model:* Another drug release kinetic model which is preferred most especially for polymer-drug release systems is Higuchi model. This model has also some assumptions which are listed below:
    - Pseudo-steady approach
    - Edges are negligible
    - The thickness of the carrier is bigger than drug particles
    - Dissolution and the swelling behavior of the polymer system are neglected.

The Higuchi model expressed by using equation given below where KH is the Higuchi model dissolution constant. By evaluating the slope of cumulative drug release percentage versus square root of time graph, KH can be found.

$$\frac{M_t}{M_0} = K_H t^{1/2} \qquad \text{(Eqn 3.8)}$$

- *Korsmeyer-Peppas Model (The Power Law):* This model is a semi-empirical model which is applied to the 60% of cumulative released drug. By calculating the slope of log (Mt/M∞) versus log(time), n can be found which defines the Korsmeyer-Peppas mechanism. Different n values represented in the Table 3.1 and depending on the geometry of drug carrier the release mechanism is determined.

$$\frac{M_t}{M_\infty} = Kt^n \qquad \text{(Eqn 3.9)}$$

Table 3. 1. Release kinetic exponent

Release Exponent (n) of different geometries			**Release mechanism**
Thin Film	Sphere	Cyinder	
n ≤ 0,5	n ≤ 0,45	n ≤ 0,43	Fickian diffusion
0,5<n<1	0,45<n<0,89	0,43<n<0,85	Anomalous diffusion or non-Fickian diffusion
n ≥1	n ≥0,89	n ≥0,85	Case-II transport

3.5.14. Antimicrobial Test

Antimicrobial test of drug loaded HNTs-zein nanofiber coated chitosan sponges were analyzed with disc diffusion method by using two different microorganisms as *Escherichia coli (E. coli*), gram negative bacteria and *Staphylococcus epidermidis* (*S.epidermidis*), gram positive bacteria. To determine antimicrobial activity of bilayer wound dressings, frozen bacteria stocks were activated overnight at 37ºC. After activation of microorganisms, 0,5 McFarland turbidity was measured in phosphate-buffered saline (PBS) solution. After that, PBS adjusted at 0.5 McFarland was streaked onto Mueller-Hinton agar plates. Empty discs with a diameter of 14 mm were placed on inoculated agar. Vancomycin release fluids collected after 24 hours, and 3 days were dripped onto blank discs (Oxoid™) as 20 µl. As control antibiotic Amoxicillin and vancomycin antimicrobial susceptibility discs (10 µg/ml 1, Oxoid™) were placed. The discs, on which the release liquids were dripped, were incubated at 37 ◦C for 24 hours. Disk diffusion test was performed in 3 repetitions for all groups. After the test was completed, the transparent areas around the discs were measured with a ruler and recorded as the zone area by making triple replicates.

3.5.15. Statistical Analysis

In this thesis experimental data were evaluated by expressing mean ± standard deviation (SD). The differences between the sample groups were analyzed by using Analysis of Variance (ANOVA) with GraphPad software.

CHAPTER 4

RESULT AND DISCUSSION

4.1 . Characterization of Halloysite Nanotubes (HNTs)

4.1.1. Morphology of HNTs

The morphology of HNTs were analyzed by SEM analysis which was shown in Figure 4. 1. According to AFM image of HNTs shown in Appendix B (Figure B.1.) the tube length was found as 454±81 nm where outer tube diameter was measured as 48±7 nm. The results indicated that HNTs had hallow tube structure with the average length of 500 nm and the average external tube diameter of 50 nm (Lvov & Abdullayev, 2013). Our results is in good agreement with the literature findings.

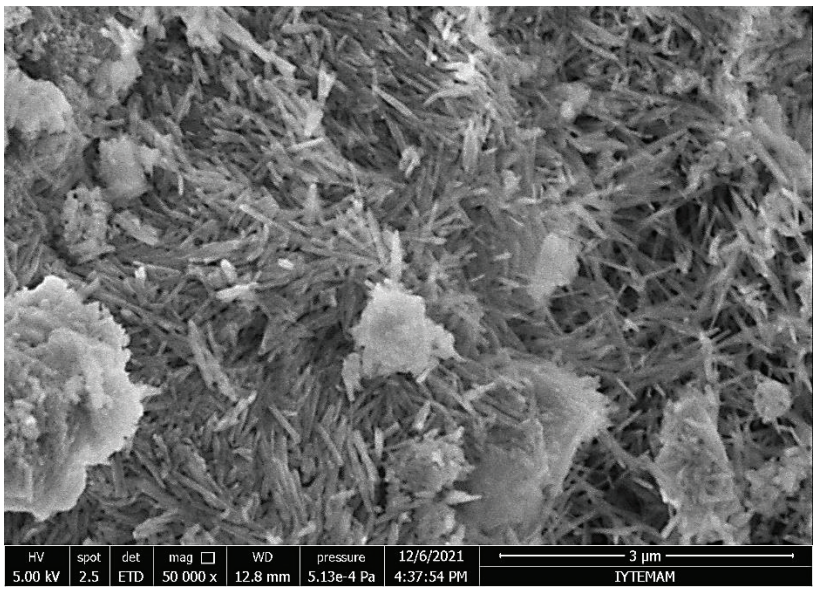

Figure 4. 1. SEM images of HNTs

4.1.2. FTIR Analysis of HNTs

Fourier-Transformed Infrared Spectroscopy Analysis of HNTs were made in between 400 to 4000 wavelength and the absorbance data was drawn with respect to wavelength. The FTIR result was shown in Figure 4. 2.(a) which contains pristine

HNTs, and drug loaded HNTs. The specific characteristic bands were listed in Table 4. 1. It was observed that the bands at 3693 cm^{-1} and 3622 cm^{-1} were assigned to the Al-OH stretching vibrations. At wavelength of 1645 cm^{-1} hydroxyl group found. Si-O-Si bond was observed at 1000 cm^{-1}. Besides, 907 cm^{-1} and 749 cm^{-1} picks relates the O-H bending of Al-OH and O-H bending Si-O-Al external vibration respectively (Pavliňáková et al., 2018). However, the vancomycin loaded HNTs did not showed any Vancomycin related bands. The FT-IR spectrum of Vancomycin showed characteristic peaks at 1652 cm^{-1} C=O stretch, 1558 cm^{-1} amide II (C-N-C), 1506 cm^{-1} (C-C) and 1231 cm^{-1} phenolic hydroxyl groups which are shown in Figure 4.2.(b) (Zhou et al., 2011). There were no differences obtained between the spectrum of drug loaded and the neat HNTs powders. This could be due to the low encapsulation efficiency of drug in HNT.

Table 4. 1 Characteristic bands of HNTs

No	Wavelength (cm^{-1})	Band	Formulation
1	3693	Al-OH	HNT
2	3622	Al-OH	HNT
3	1645	-OH	HNT
4	1000	Si-O-Si	HNT
5	907	OH- bending of Al-OH	HNT
6	749	OH- bending of Si-O-Al	HNT

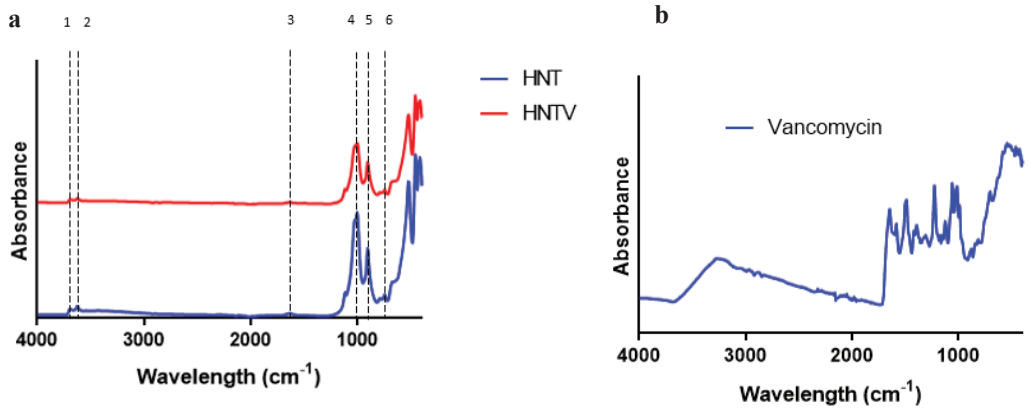

Figure 4. 2. FTIR Spectra of HNTs and Vancomycin-loaded HNTs (a) and Vancomycin (b)

4.1.3. Zeta Potential of HNTs

Zeta potential of HNTs was investigated at various pHs. It was seen that zeta potential varies depending on the pH values of solution. In this study, 3 different pH values were selected to observe the change of HNTs surface charge as seen in Figure 4. 3. Zeta potential of HNTs at pH 3, 5 and 8 was found as -9,69, -21,07 and -21,53 mV respectively. These values were changed to -9,68, -11,94 and -21,38 mV for the drug loaded HNTs which were shown in Table 4. 2. As seen in graph, zeta potential decreased with an increase of pH values. Since vancomycin has positive surface charge, it was evident that vancomycin was not only encapsulated into the HNTs lumen but could also connected to outer surface of HNTs.

Johnson et al., investigated surface charge of Vancomycin at different pH's and they observed that vancomycin has a positive surface charge and isoelectric point at pH 8,3 (Johnson & Yalkowsky, 2006). . Increasing pH values of vancomycin from 3 to 8,3 results in decreasing surface charge. Since HNTs surface charge at pH 3 is higher than 5 and 8, the change of surface charge was not found significant. When pH was increased to 5, surface charge of HNTs decreased more significantly than pH 3. Therefore, the drug loaded and unloaded HNTs have high differences. The differences decreased at pH 8 for drug loaded and unloaded HNTs since vancomycin has isoelectric point at pH 8,3.

Pan et al., evaluated the zeta potential of HNTs for different pH values. They also found that the zeta potential of HNTs was negative at all pHs. According to their study, isoelectronic point of HNTs was observed at pH 1 and the zeta potential of HNTs was decreasing with the increasing pH values. Also, vancomycin drug loading slightly increases the zeta potential since vancomycin has positive surface charge (Pan et al., 2017). Avani et al., also studied the surface charge of HNTs, and vancomycin loaded HNTs. They found that zeta potential of HNTs and vancomycin was -24,3 and +23,6 Mv respectively. After loading of vancomycin, this value became -20.1 mV. Therefore, HNTs surface charge was changed with the loading of vancomycin (Avani et al., 2019). Our findings were found in agreement with the literature.

Table 4. 2. Zeta potential values at different pHs for HNT and Vancomycin loaded HNTs Powder

	pH = 3	**pH = 5**	**pH = 8**
HNT	-9,69 ± 0,94 mV	-21,07 ± 0,58 mV	-21,53 ± 0,33 mV
HNTV	-9,68 ± 0,79 mV	-11,94 ± 0,34 mV	-21,38 ± 0,39 mV

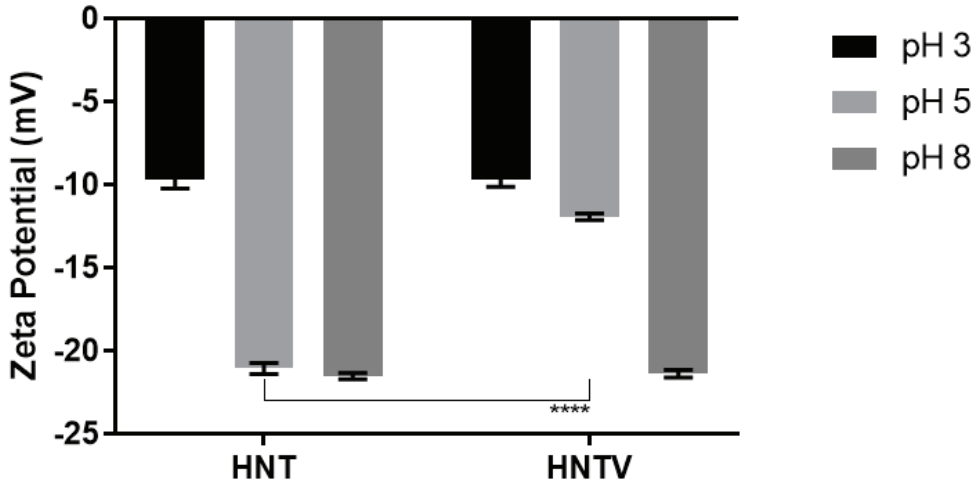

Figure 4. 3. Zeta potential change of HNTs and vancomycin loaded HNTs in different pH values.

4.1.4. Encapsulation Efficiency

Encapsulation of vancomycin drug into HNTs was provided by vacuum method. The effects of sonication and microfluidics processes on the encapsulation and loading efficiency of drug were investigated. Table 4. 3 shows encapsulation and loading efficiencies of vancomycin drug for different HNT:drug ratios. The highest encapsulation efficiencies were obtained in the range of 23-26% for both homogenization techniques. It was seen that the higher HNT loading enhanced the encapsulation efficiency from 14,21 to 26,12% with an increase of HNT from 1 to 5 wt%. However, HNT:drug ratio of 1:1 gave the lowest encapsulation efficiency. Also loading efficiencies were found similar for both microfludix and ultrasonication homogenization processes. According to the encapsulation efficiency results, microfluidics process was selected for further steps, since it had slightly higher encapsulation efficiency than sonication process especially for

higher amount of HNTs as 5wt%. Avani et al., fabricated vancomycin loaded HNTs embedded in silk fibroin hydrogel used for bone tissue engineering. By increasing HNT from 1 to 100 mg in the drug solution which contains constant vancomycin amount as 10 mg, encapsulation efficiency was increased from 5 to 47%. Besides it was found that increasing of vancomycin amount from 5 to 100 mg at constant HNTs loading as 10 mg, encapsulation efficiency was decreased from 25 to 19%. However they selected moderate amount of HNTs to prevent agglomerations (Avani et al., 2019). Therefore, based on the efficiency results, in this study the optimum loading ratio of Vancomycin-HNTs was selected as 1:2 and 1:5. For further studies related to the fabrication of the upper layer of bilayer dressing and characterization of the dressing, these ratios were used. Vancomycin drug release was also investigated for both HNT:drug loaded samples.

Table 4. 3. Encapsulation efficiency and loading efficiency of vancomycin into HNTs by using two different processes

Drug: HNTs ratio	**Encapsulation efficiency by using sonication**	**Encapsulation efficiency by using microfluidics**	**Loading efficiency by using microfluidics**
1:1	14,64 %	14,21 %	14,6 %
1:2	24,33 %	23,35 %	12,2 %
1:5	23,52 %	26,12 %	10 %
2:1	24,69 %	23,61 %	15 %

4.2. Characterization of Zein-HNT Nanofiber (Upper Layer)

4.2.1. Morphology of Zein-HNT Nanofiber Layer

In this study zein-drug loaded HNT nanofibers were produced as upper layer. In nanofiber formation, effects flow rate and HNT concentration on the morphology of zein -HNT nanofibers were investigated to have uniform fiber morphology. Electrospinning was carried out under constant voltage of 20 kV and constant distance of 10 cm with varying flow rates and HNT loading amounts. Previous studies related to zein spinnability was investigated by several researchers. It was found that 25 wt% zein concentration is

optimum for having uniform diameter and bead/ wrinkle free morphology (Gunes et al., 2020; Adhirajan et al., 2009; Dashdorj et al., 2015; Kimna et al., 2018; Ullah et al., 2019). Nanofiber diameters were calculated by using Image J program. SEM image of pristine zein was shown in Figure 4. 4 which has an average fiber diameter of 578 ± 0,16 nm. In the study of Gunes and coworkers, it was found that the zein nanofiber layer has an average fiber diameter of 550 ± 0,03 nm which was found quite similar to our findings.

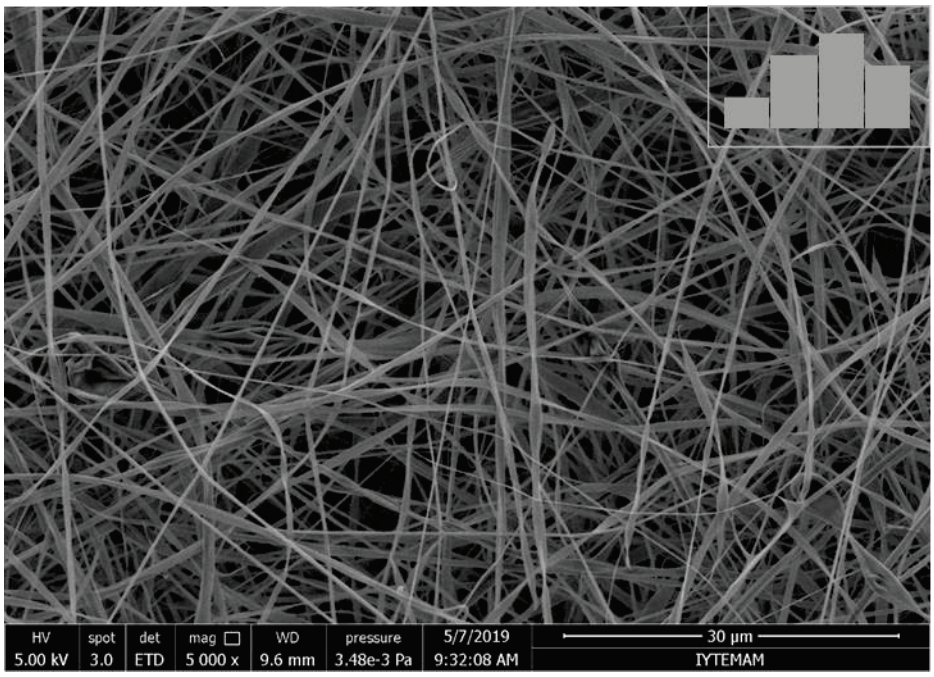

Figure 4. 4. SEM Image of zein nanofiber.

Figure 4.4 shows the morphology of the fabricated pure zein and zein-HNT nanofibers (1wt% HNT) with varying flow rates of 1-10ml/h. As seen from the Figure 4. 5 and Table 4. 4, the higher flow rates above 3 ml/h caused bead formation as well as non-uniform fiber morphology. Bead free fiber morphology was obtained between the flow rate of 1-3 ml/h.

Table 4. 4. Effect of flow rate on nanofiber formation

Groups	Flow Rate (ml/h)	Bead Formation
1	1	No beads
2	2	No beads
3	3	No beads
4	5	Beads observed
5	7	Beads observed
6	10	Beads observed

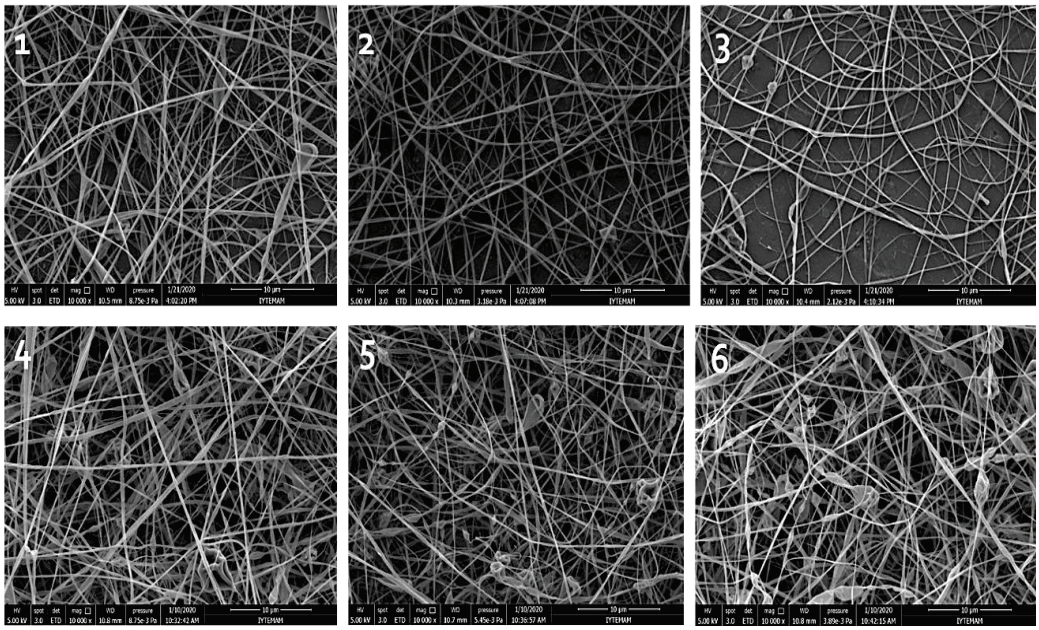

Figure 4. 5. SEM images of electrospun zein and zein nanofibers (1 wt% HNT loaded) with varying flow rates

Since the bead formation is occurred above 5 ml/h flow rates, the further experiments were carried out in the range of 1-5 ml/h.

Effects of HNT incorporation and HNT concentration on morphology and diameter of fiber were investigated and illustrated in Figure 4.6 and Table 4.5 with varying flow rates. SEM pictures showed that when the flow rate is increased, fibers have un- even (non-homogenous) and smaller diameter in size. The average of at least 50 fiber diameters of each sample was measured. The average diameters of 1 wt % HNT loaded zein fibers changed from 405 to 367 nm with increasing flow rates. Addition of HNT into zein also decreased the average fiber diameter. As HNT loading is increased from 1 wt% to 5wt%, the average fiber diameter decreased from 404 to 360 nm. Our result is in agreement with the findings of Yilmaz and coworkers (Yilmaz et al., 2020).

Table 4. 5. Effects of flow rate and HNT loading on fiber diameter.

Groups	**Flow Rate (ml/h)**	**HNT Concentration (wt%)**	**Nanofiber Diameter (nm)**
1	1	1	404,78 ± 0,06
2	3	1	378,42 ± 0,04
3	5	1	367,00 ± 0,05
4	1	3	400,20 ± 0,05
5	3	3	358,60 ± 0,04
6	5	3	335,50 ± 0,04
7	1	5	360,70 ± 0,05
8	3	5	360,12 ± 0,07
9	5	5	333,75 ± 0,07

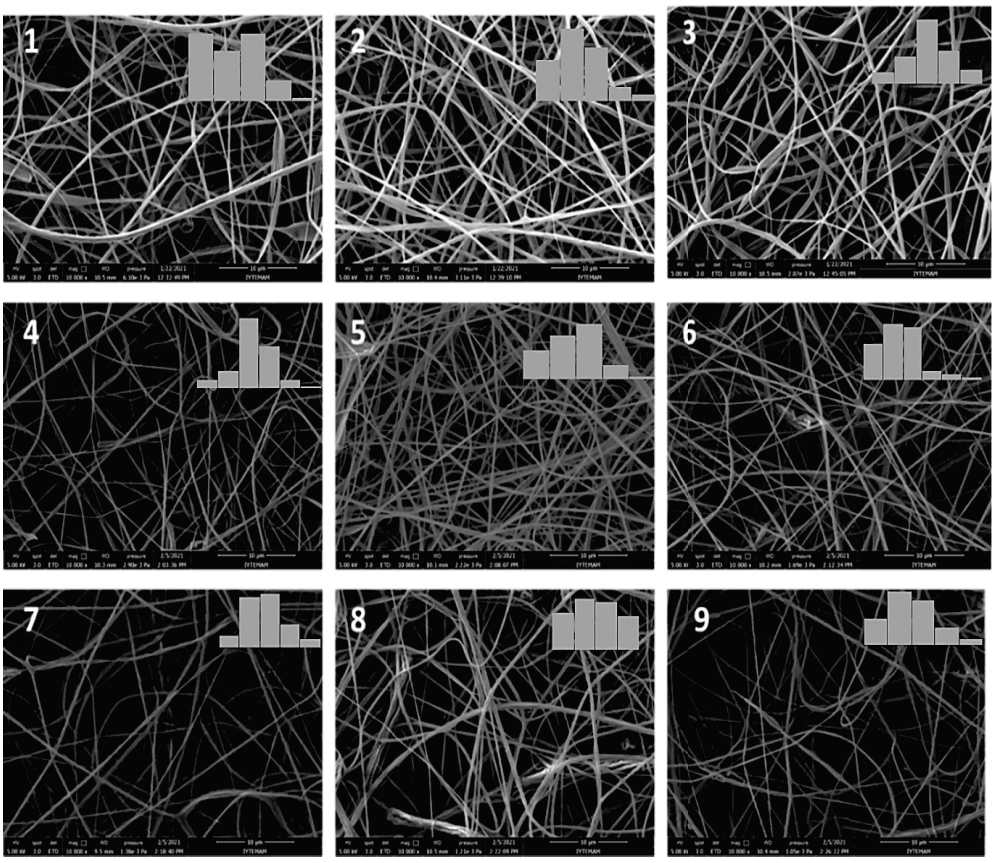

Figure 4. 6. SEM images of electrospun of Zein-HNT nanofibers

5 wt % loaded nanofibers have much higher standard deviation as ± 0,06, so fiber diameters were not homogeneous as found for 1 and 3 w t% HNT loaded nanofibers. This can be explained with the formation of thick and fine nanofibers due to agglomeration of HNTs. According to all SEM images, nanofiber processing parameters were set as 10 cm distance, 20 kV voltage and 3ml/h flow rate for further processes. Also, HNT concentration was fixed as 3 wt% for drug loading studies.

In literature Dong et al., fabricated polylactic acid (PLA) and HNT electrospun mats by changing HNTs content as 1,5 and 10 wt%. They found that addition of HNT content did not influence on the average fiber diameter (Dong et al., 2015). However, Yılmaz and his coworkers observed a decrease of fiber diameter with the addition of HNT and agglomerations with an increase of HNT from 0,5 to 5 wt%. This result indicates that electrical conductivity of the electrospinning solution increased with the inorganic additives which result higher electrostatic forces and higher surface charge density (Yilmaz et al., 2020). Also, in the study of Pavliňáková and coworkers, non-homogenous fiber structures were obtained due to agglomerations from 3 wt% to 9 wt% (Pavliňáková

et al., 2018). Our result has similar finding with Yılmaz et al., (2020) regarding to nanofiber diameter change with HNT addition.

Morphology of drug loaded HNT-zein nanofibers were also analyzed by SEM with various HNT loading (1-5 wt%) while keeping 3 ml/h flow rate, 10 cm distance and 20kV voltage constant as seen in Figure 4. 7. There were no morphological differences observed between drug loaded or unloaded HNT-zein nanofibers. Also, the average fiber diameters were calculated and shown in Table 4. 6. With the increasing HNT concentration, fiber diameters did not change significantly, however slightly increased from 202,7 nm to 225.2 nm with the addition of 5 wt % of drugs loaded HNT. In addition, it was also observed that the standard deviation was found larger for 5 wt% HNT loading.

The average diameters of the drug loaded HNT-zein nanofibers fabricated in this study were found in the appropriate range of the diameter of native skin tissue fibril that varies between the range of 50-500 nm (Barnes et al., 2007).

Table 4. 6. Average fiber diameter of drug loaded HNTs.

Groups	**HNT Concentration (g/ml)**	**Nanofiber Diameter (nm)**
a	1	202,7 ± 0,05
b	3	214,3 ± 0,03
c	5	225,2 ± 0,06

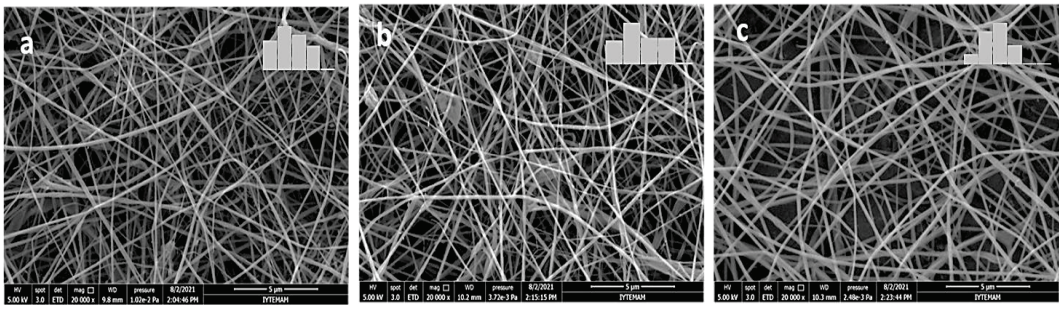

Figure 4. 7. SEM images of the drug loaded HNT-zein nanofibers (a 1wt%, b 3 wt%, c 5 wt% Drug-HNT ratio 1:5)

4.2.1. FTIR Analysis of Zein-HNT Nanofiber Layer

Chemical structure of the Zein-HNT fibers and interaction between Zein and HNT was investigated by using attenuated total reflection attachment (ATR)-FTIR equipment. FTIR spectrum of the fibers were depicted in Figure 4. 8. The characteristic bands of the nanofibers were also given in Table 4. 7. Zein has specific peaks at 3292 cm-1, 1643 cm^{-1}, 1531 cm^{-1} and 1240 cm^{-1} which represent the -NH2 stretching, amide I, II, and III bonds, respectively (Ali et al., 2014). The presence of HNT in Zein nanofibers was proven with its characteristic peaks at 1115 cm^{-1} that represents the Si-O-Si bond (Ali et al., 2014 ; Pavliňáková et al., 2018).

Table 4. 7. Characteristic bands of Zein and HNTs incorporated Zein fibers.

No	Wavelength (cm^{-1})	Band	Formulation
1	3292	-NH2 Stretching	Zein
2	1643	Amide I	Zein
3	1531	Amide II	Zein
4	1240	Amide III	Zein
5	1115	Si-O-Si	ZHNT1, ZHNT3, ZHNT5

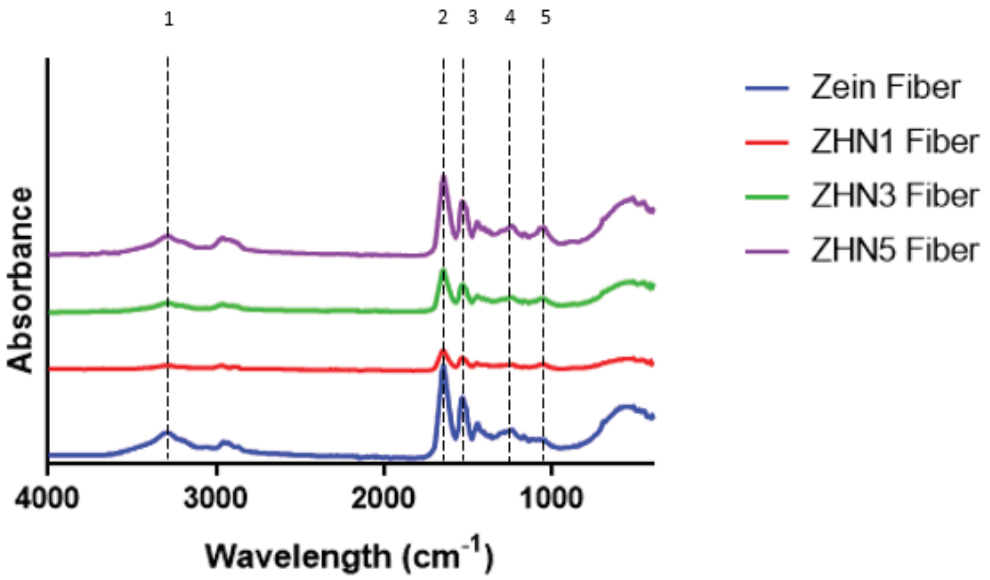

Figure 4. 8. FTIR Spectra of zein and zein-HNTs fibers

4.2.2. Thermogravimetric Analysis of Zein-HNT Nanofiber Layer

Thermogravimetric analysis of pure zein nanofiber and zein-HNT nanofibers with different HNT loading (1, 3 and 5 wt%) was shown in Figure 4. 9. The first weight loss occurred between 50-60°C due to removal of water and volatile compounds. The second step of weight loss was appeared at 260-550°C due to thermal degradation of zein. This degradation step is caused due to the breakage of amino acid breakdown and peptide cleavage. The final weight loss is observed between 550-770°C.

Mariotti el al., found that the first mass loss step of zein occurs between 50-200°C due to water vaporization and removal of volatile compounds (Mariotti et al., 2020). The main zein thermal degradation occurred at 280-450°C. The final degradation step was reported as between 570 and 660 °C. Our result was found in agreement with the findings of Mariotti and coworkers.

As seen in the Figure 4. 9, addition of HNT delayed the thermal degradation temperature of zein from 600°C to 780°C. Gorrasi et al., evaluated that the thermal degradation of neat zein film and HNTs added zein film. They investigated thermal degradation of the films, however the thermal degradation was investigated under N_2 atmosphere in our study. They found that the first degradation occurs at 80°C due to loss of moisture. The second step at 230°C to 380°C due to the cleavage through amino acid

and peptide bond. The final decomposition of the films was observed at 430-630°C. It was found that the addition of HNTs into zein film prevent the third decomposition step of the material compared to zein (Gorrasi & Vertuccio, 2016).

Figure 4. 10 illustrates the effect of drug on thermal degradation behavior of Zein-HNT fibers and compares with the pure zein fibers. It was seen that the addition of drug loaded HNTs delayed the degradation of zein fiber after 500°C compared to unloaded Zein-HNT fibers, however in nanocomposite fibers, degradation is fastened between 400-600°C, then it is delayed compared to the unloaded composite fibers and pure zein fibers. Pan et al., studied the weight loss of HNTs and vancomycin loaded HNTs in the temperature range of 37 to 770°C. It was seen that, vancomycin loaded HNTs was degraded much faster than pristine HNTs due to loading of drug (Pan et al., 2017).

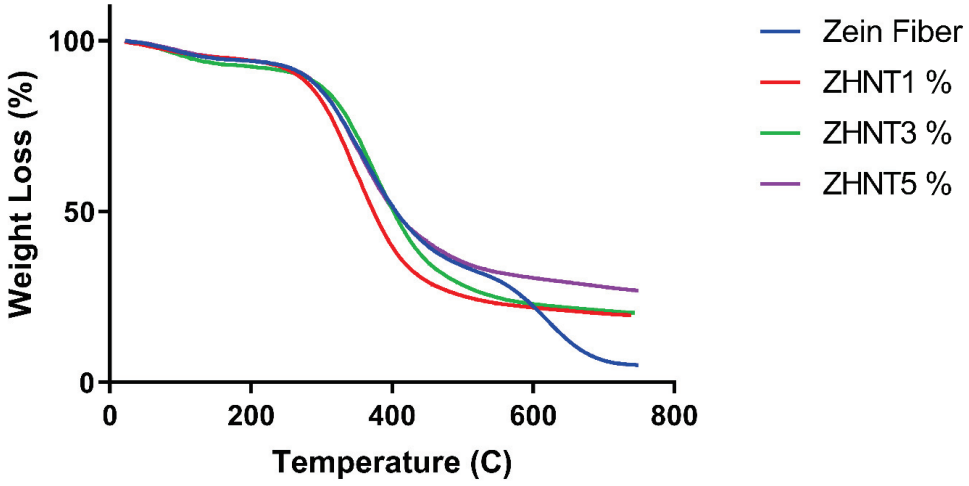

Figure 4. 9. TGA results of Zein and Zein-HNT fibers

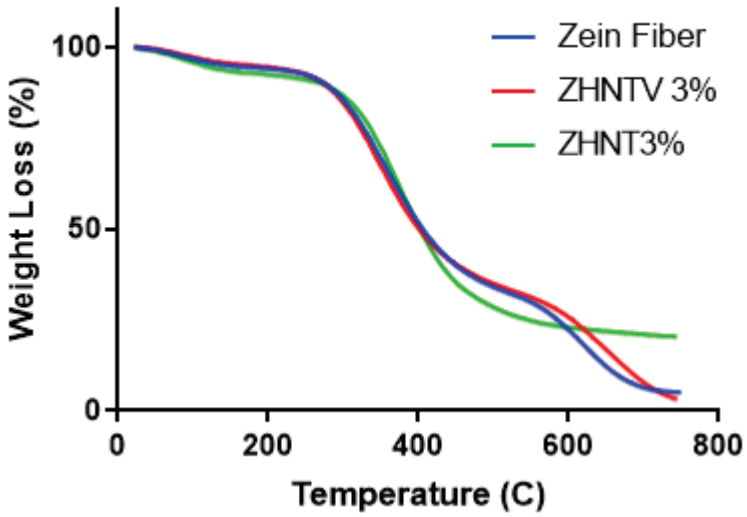

Figure 4. 10. TGA results of Zein, Zein-drug loaded and unloaded HNT fibers

4.2.3. Contact Angle Measurement of Upper Layer

The static air-water contact angle was conducted to determine the structure wettability behavior of the upper layer which consist of zein-HNT nanofibers by dropping 5 µl ultrapure water onto dried fibers. Results showed that neat zein (25wt%) nanofiber mats had moderately hydrophobic character since it has nearly 91°contact angle with a standard deviation of ±1,21 (Yuan et al., 2017). However, it was found that addition of HNTs into zein fiber loading showed lower contact angles with a moderately hydrophilic characteristic when compared to pure zein nanofibers as in the range of 84-71 ° for 1 to 5 wt% HNT loading (Figure 4. 11 and Table 4. 8). Therefore, it is evident that the addition of HNTs into zein matrix improved the hydrophilic behavior of zein polymer which is preferable for tissue engineering applications for better cell adhesion and water uptake. In the study of Zou et al., they fabricated chitosan/polycaprolactone (CS/PCL) nanofibers containing different amount of HNTs. It was observed that the PCL/CS nanofiber had nearly 109° contact angle. Addition of 6 wt% HNT decreased contact angle to 52° due to the presence of polar hydroxyl groups (-OH) of HNTs (Zou et al., 2020). According to the results, there is a significant difference between the contact angles of pure zein and Zein containing 3 wt% HNT and 5 wt% HNT zein nanofibers. Contact angle values of vancomycin loaded HNT-zein nanofibers were also investigated. In Figure 4. 12, it was seen that the vancomycin drug loaded HNTs showed lower contact angle than unloaded-

HNTs. The contact angle decreased to 80°, 64° and 63° for 1 wt % (HNTV1), 3 wt% (HNTV3), and 5 wt% (HNTV5) HNT loading respectively. (Drug:polymer ratio 1:5) The significant differences were observed in between Zein vs. Zein-HNT (3 wt%) and zein vs Zein-HNT (5 wt%) samples respectively. (**)

Contact angle images of pure zein and drug loaded 3wt%HNT-zein nanofibers were also illustrated in Figure 4. 13. As seen the contact angle of zein decreased from 91 to 64°. Yu and coworkers also found that addition of vancomycin drug into polycaprolactone (PCL) scaffold increased hydrophilicity as 69° (Yu et al., 2020). In this study, the fabricated bilayer wound dressing, showed more hydrophilic character with the incorporation of drug into HNTs which is appropriate for wound dressing application.

Table 4. 8. Contact angle results of Zein, Zein-HNT and Zein-drug loaded HNT fibers

Groups	Contact Angle
Zein	91° ± 1,2
ZHNT 1%	84° ± 2,4
ZHNT 3%	75° ± 7,2
ZHNT 5%	71° ± 2,6
ZHNTV 1%	80 ± 2,9
ZHNTV 3%	64 ± 5,9
ZHNTV 5%	63 ± 2,9

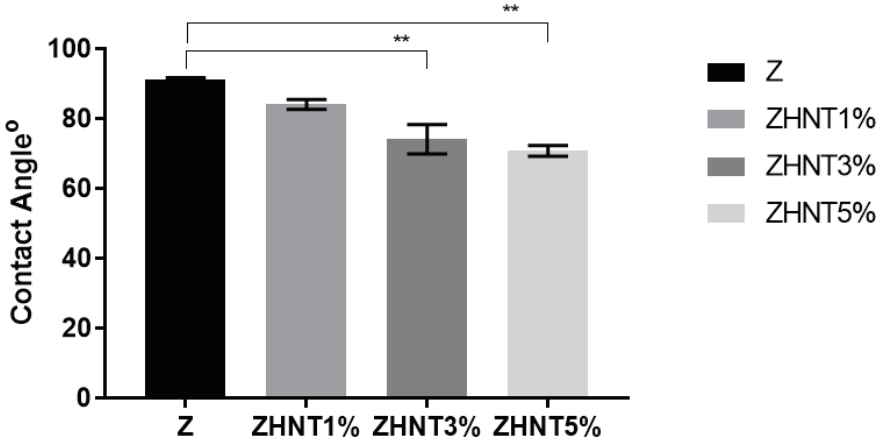

Figure 4. 11. Contact angle of pure Zein and Zein-HNTs fibers

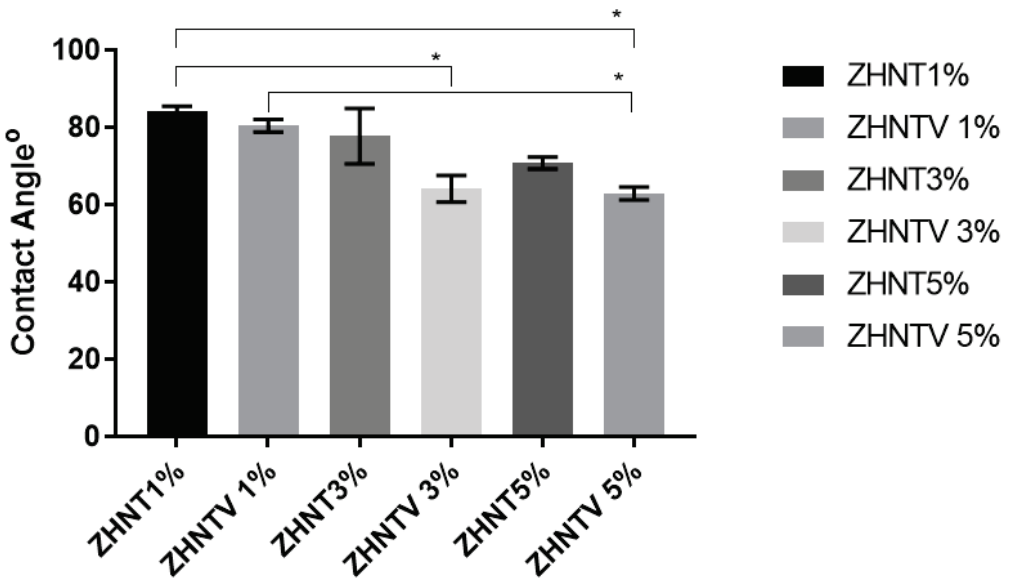

Figure 4. 12. Contact angle of unloaded and drug loaded HNTs - zein nanofibers

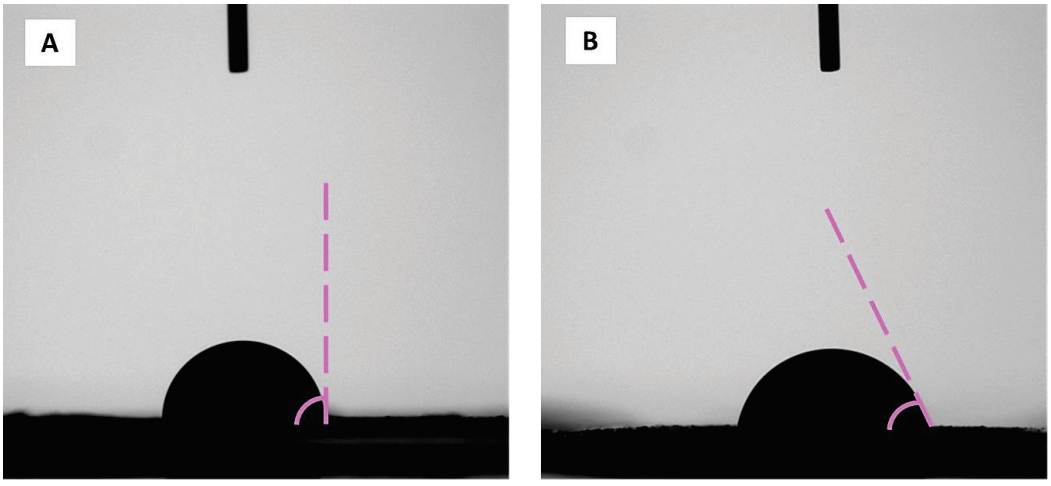

Figure 4. 13. Contact angle images of zein nanofiber (A (91°) and zein HNTV3 nanofiber (B) (64°)

4.3. Morphology of Bilayer Wound Dressing

The lower layer contains chitosan porous sponges, and it had an average pore diameter of 51,8 ± 14,19 nm which was shown in Figure 4. 14 . Average pore size of the sponge was measured by using Image J software with at least 50 points. In the study of Tamburaci et al., average pore size of chitosan sponge was found as 70,7 ± 0,04 nm for bone tissue application (Tamburaci & Tihminlioglu, 2021). In another study of Ikeda and

coworkers, they fabricated chitosan sponges at different concentration of chitosan and investigated the effect on microstructure. It was found that the 2 wt% chitosan sponge has an average pore size of 74,5 (Ikeda et al., 2014). The slight changes in pore sizes could be due to the differences of chitosan molecular weights and preparation parameters.

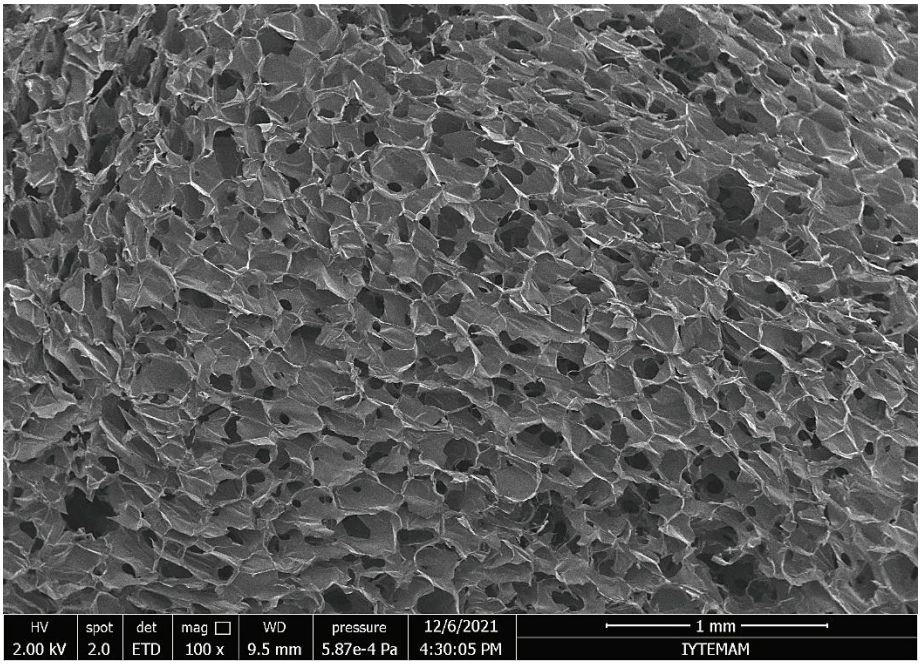

Figure 4. 14. SEM image of Chitosan (2 wt%) sponge.

Figure 4. 15 and Figure 4. 16 showed the cross-sectional representation of bilayer wound dressings. As seen in the Figure 4. 15, vancomycin loaded HNTs (3%wt) -zein nanofibers were uniformly coated on the surface of chitosan sponges and adhered well on the chitosan sponge. The zein (25wt %) containing vancomycin loaded HNTs (3wt %) nanofibers were matched well with the pores of the chitosan sponge (2wt%). Fiber thickness was measured as 110 ± 8,9 μm for 4 ml coating of electrospun fibers.

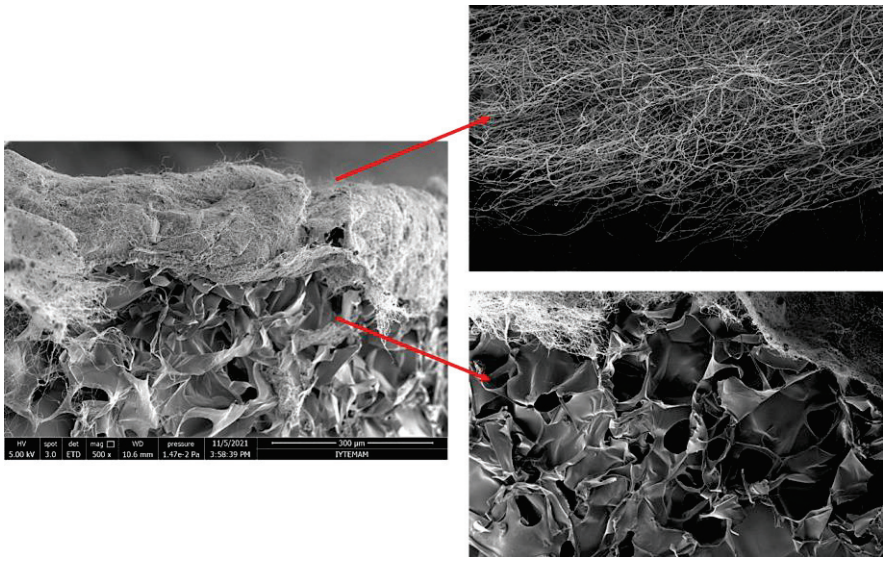

Figure 4. 15. Cross sectional representation of bilayer wound dressing

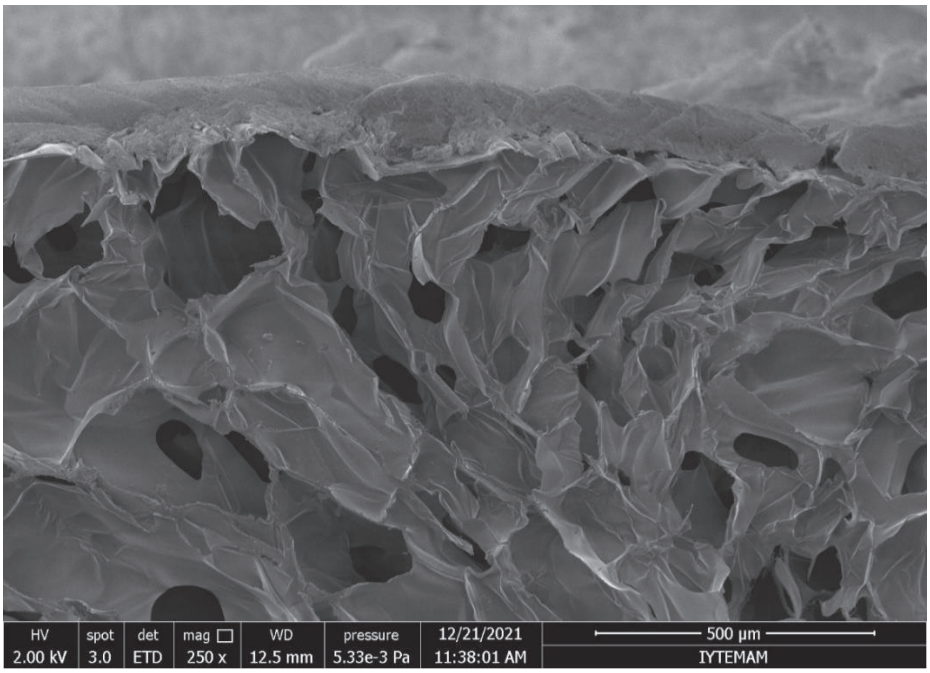

Figure 4. 16. SEM image of bilayer wound dressing

4.4. Porosity % of Mono & Bilayer Wound Dressings

Open porosity was measured for monolayer chitosan sponge and zein-3% HNT nanofiber coated chitosan sponge with as 70,9 % ± 0,8 and 66,1 % ± 0,9 which were shown in Table 4. 9. Porosity of the bilayer wound dressing was decreased with the

nanofiber layer. Tamburaci et al. fabricated Si doped low molecular weight chitosan sponges with an open porosity of 73-80% (Tamburaci & Tihminlioglu, 2021). Ikeda et al., found that 2wt% of chitosan sponge as 80.2% (Ikeda et al., 2014). . Anisha et al., prepared chitosan–hyaluronic acid/nano silver sponges for diabetic wound and the porosity was found as 63 %. Therefore, chitosan sponge had approximately similar porosity percentages.

Table 4. 9. Porosity percentages of Chitosan and Chitosan coated Zein-HNT (3 wt%) Nanofiber

Groups	**Porosity %**
CHI	70,9 % ± 0,8
CHI-ZHNT 3%	66,1 % ± 0,9

4.4. Characterization of Bilayer Wound Dressing

4.4.1. Mechanical Test

Mechanical properties of bilayer wound dressings were observed by 75% compression test. Compression strength and Young's modulus were measured and shown in Figure 4. 17 and Figure 4. 18 respectively. Compression strength means that the maximum stress of bilayer wound dressings had per unit area (mm^2). Sponges were measured with 20 mm of diameter and 10 mm of height. The unit area of sponges was set as 314 mm^2. Also, Young's modulus or elastic modulus (E) represents that the stiffness of material and can be calculated by taking slope of stress-strain curve.

As seen in the graphs, compression strength values of both mono layer and bilayer dressing were shown. The effect of coating amount (2ml and 4ml) on the monolayer was also investigated on the compression strength and the Young's modulus values. It was found that the compression strength of neat low MW chitosan sponge had 130,33 kPa value, however the addition of zein fiber layer increased the compression strength from 130,33 to 145,33 kPa. The incorporation of 1-5wt% of HNTs into zein fiber enhanced the strength values further in the range of 148-149 kPa. Since the fiber thickness was very small (55 ± 4) for 2ml coating with respect to the sponge thickness, the effect of HNTs

addition was not observed on the results. However, when 4 ml polymer coating solution was electrospun and the fiber thickness found as 110 µm, and the maximum compression strength was observed for 5 wt % HNT as 164 kPa. It can be concluded that the incorporation of HNT enhanced the compression strength. Gorrasi et al., studied that environmental friendly zein incorporated HNTs films for food packaging and they found that increasing of HNT filler content to 3 wt% increased the tensile stress at break (Gorrasi & Vertuccio, 2016). In the study of Shi et al., gelatin elastomer nanocomposite membranes were enhanced by addition of drug loaded HNTs with a content of 0, 5, 10, 15 and 20 wt% for wound healing applications. They also observed that the addition of HNTs filler content in gelatin elastomer matrix increases the compression strength of membrane (Shi et al., 2018).

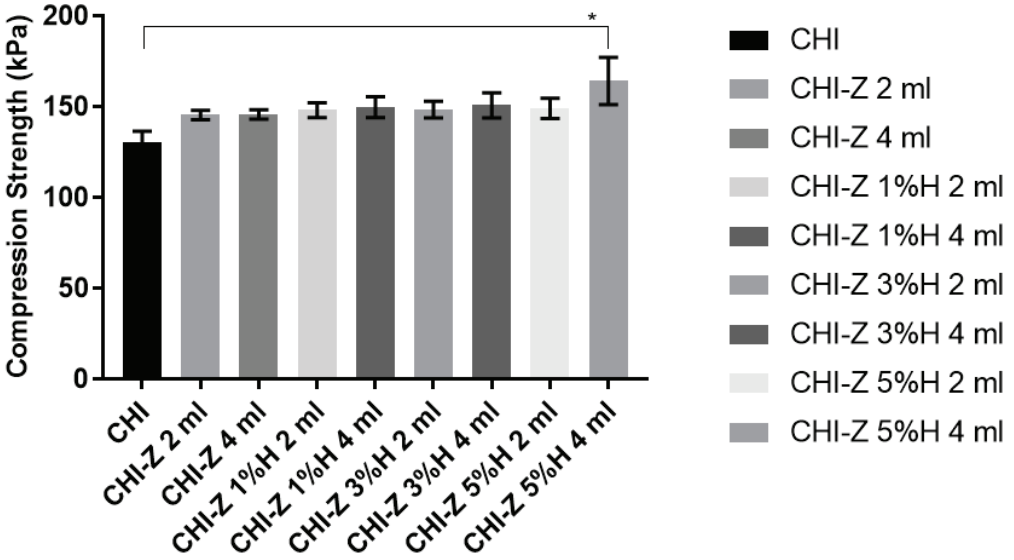

Figure 4. 17. Compression strength of one and bilayer wound dressings.

Young's modulus of one and bilayer wound dressings were also enhanced by addition of halloysite nanotubes shown in Figure 4.18. The Young's modulus of neat chitosan sponge was found as 1,60 kPa. Değer et al., also prepared chitosan sponge for wound dressing and they found the Young's modulus of mono layer chitosan sponge as 1,88 kPa (Değer, 2019). Zein fiber layer increased the modulus of material to 2,07 kPa. Incorporation of 1-5 wt% HNT into zein fiber enhanced the Young's modulus of the bilayer dressing range of 2,17-3,03 kPa for 2 ml coating. When the fiber thickness became doubled, the values were found almost similar except 5 wt% HNT loading, the modulus

increased to 3,8 kPa. As a result, the bilayer dressing has much higher compression strength and young's modulus compared to single layer.

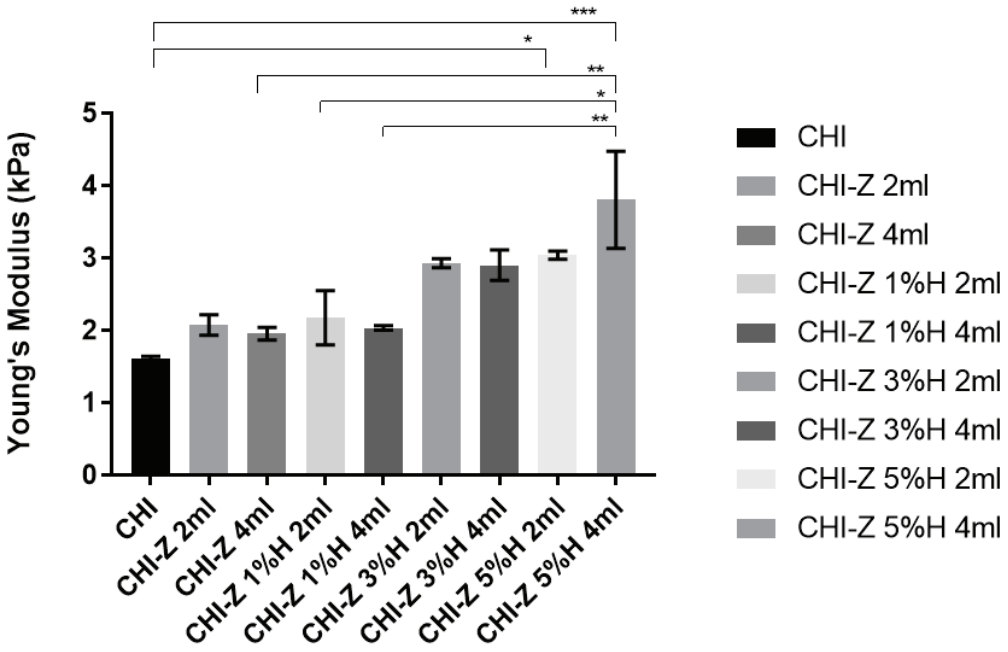

Figure 4. 18. Young's modulus of one and bilayer wound dressings.

4.4.2. Water Vapor Permeability

Water vapor permeability is an important parameter for wound dressing applications. The wound should have ideal humid environment to prevent drying around wound site. The human skin has water vapor permeability of 204 g/m^{2}day (S. Patel et al., 2018). In this study, water vapor permeabilities of three different groups were measured. Respectively one layer chitosan sponge, chitosan-zein 3 wt.% HNT nanofiber bilayer and drug loaded bilayer wound dressings have 4102, 2833 and 2409 g/m^{2}day water vapor transmission rates which were shown in Table 4. 10. Since wound dressings should have permeability value from 279 to 5138 g/m 2day with respect to wound type the groups have all provides necessary skin permeability (Patel et al., 2018). Neat chitosan sponges' permeability was decreased with the addition of nanofiber layer. Thu et al., studied alginate-based bilayer film wound dressing by using ibuprofen drug. They found that with the addition of nanofiber layer, water vapor permeability was decreased since this layer closed the permeability pathways (Thu et al., 2012). Kimna et al., also investigated water vapor transmission rate of mono and bilayer wound dressings and they found that the

addition of fiber layer also reduced the transmission rate (Kimna et al., 2019). The drug loaded and unloaded HNTs-zein nanofiber wound dressings had nearly same transmission rate. Since the drug encapsulation is low, bilayer wound dressings had no effect on permeability.

Table 4. 10. Water vapor permeability of wound dressings

Samples	**WVP x10^5 (mol.min^{-1}.cm^{-1}.kPa^{-1})**	**WVTR (g.m^{-2}.day^{-1})**
CHI	3±2,2	4102±700
CHI-ZHNT3%	2,9±1,9	2833±188
CHI-ZHNTV3%	2,9±2,9	2409±237

4.4.3. Swelling Property

Water uptake capacity is an important parameter for wound dressings due to wound exudates. Swelling experiments (%) were carried out by measuring the weight change of wound dressing in 1 x PBS solution with an incubation time of 24 and 48h hours. Swelling percentages of single and bilayer dressings were shown in Figure 4. 19 and Table 4. 11. It was observed that in all groups water uptake capacity increases as the incubation time increases from 24 h to 48 h. One layer chitosan sponge had a water absorption capacity of 2417 % and 2928 % for 24 and 48h respectively. Tamburaci et al., found that swelling ratio of low MW chitosan as nearly 25 (2500 %) for 24 and 48h. This percentage was found to be in good agreement with the findings of Tamburaci et al. (Tamburaci & Tihminlioglu, 2021). Coating of chitosan sponge with pure zein nanofiber decreased the swelling percentages to 1719 and 2299% for 24 h incubation time. Since nonpolar amino acids and predominantly hydrophobic character of zein caused to lower water uptake percentage (Gorrasi & Vertuccio, 2016 ; Kimna et al., 2019). Besides, addition of HNT (3 wt%) into zein resulted in an increase in water uptake capacity of the bilayer dressing due to hydrophilic nature of halloysite nanotubes which were found as

2455 % and 2997 % for 24 and 48h respectively. Increase in swelling percentages of the bilayer dressing were obtained for 48 h incubation time compared to neat chitosan sponges. Vancomycin loaded HNTs-zein nanofiber coating showed higher water uptake capacity compared to drug free HNTs due to hydrophilic character of vancomycin (Grace, 2012). Swelling percentage of the bilayer dressing for 24 h and 48 h were 2732 % and 3048 % respectively. The higher swelling % is preferable for diabetic acute wounds to absorb the wound exudate.

Table 4. 11. Swelling % of mono and bilayer wound dressings

Groups	24 h	48 h
CHI	2417±233	2928±83
CHI-Z	1719±174	2299±878
CHI-ZHNT 3 wt%	2455±133	2997±59
CHI-ZHNTV 3 wt%	2732±94	3048±87

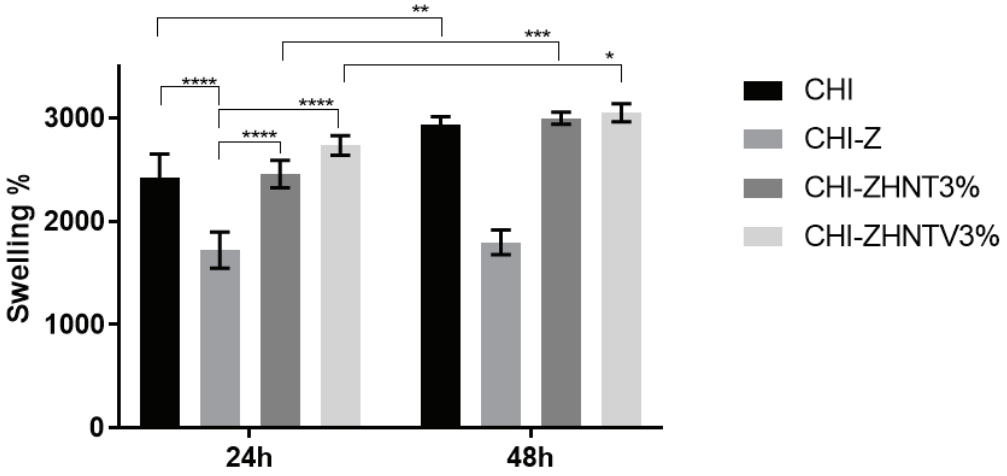

Figure 4. 19. Water uptake capacity (%) of one and bilayer wound dressings for 24 and 48 h of incubation in PBS (pH = 7.4).

4.4.4. *In Vitro* Degradation Study

Degradation of the bilayer dressing was evaluated in 1 x PBS solution with addition of sodium azide and lysozyme to mimic human blood environment at 37°C. According to degradation test, neat one layer chitosan sponge (CHI) has weight loss of

51,7 % and 58,1 % for 7 and 14 days incubation time respectively which were shown in Table 4. 12 and Figure 4. 20. Bilayer membranes containing pure zein nanofiber caused a decrease in weight loss % to nearly 21,4 and 26,2 % at the 7 days and 14 days incubation time, respectively. With the incorporation of 3 wt% of HNTs into zein nanofiber, the weight loss percentage decreased to ever lower values as 12,1 and 13,9 % for 7 and 14 days incubation times, respectively. It was found that vancomycin loading into HNT did not change the degradation % of the dressing compared to drug free HNTs in zein nanofibers. In all groups, however, degradation % was increased as the incubation time increased from 7 to 14 days. Therefore, it was evident that the addition of 3 wt% HNTs filler content helps to decrease of enzymatic degradation of the wound dressing prepared in this study. Similar findings were found in the study of Shi and coworkers for gelatin-HNT composites (Shi et al., 2018).

Table 4. 12. *In vitro* degradation % of mono and bilayer wound dressings

Groups	**7 days**	**14 days**
CHI	51,7±8 %	58,1±7 %
CHI-Z	21,4±15 %	26,2±0,1 %
CHI-ZHNT 3 wt%	12,1±0,2 %	13,9±10 %
CHI-ZHNTV 3 wt%	12±4 %	13,4±1 %

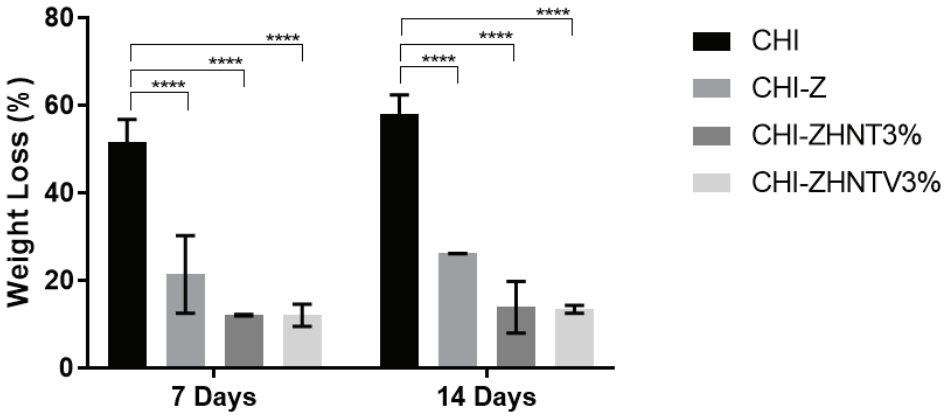

Figure 4. 20. Weight loss (%) of one and bilayer wound dressings in degradation media.

4.4.5. *In Vitro* Drug Release study

The *in vitro* release behavior of vancomycin from bilayer dressing was investigated and depicted in Figure 4. 21. Bilayer dressing containing Zein-vancomycin fiber (drug dispersed in zein-HNTs matrix), Zein-HNTs-Vancomycin nanofiber (HNT and Vancomycin were dispersed into zein solution) and Vancomycin loaded HNT-zein fibers with two different drug:HNT ratios (1:2 and 1:5) were used in order to monitor release behavior of drug in PBS at pH=7.4. As seen in the Figure 4. 21, fast burst release of vancomycin from zein fibers was obtained. Also, the cumulative drug release profile of vancomycin loaded HNT-zein fibers at 1:2 and 1:5 drug:HNT ratios during14 day was shown in Figure 4. 22. Total amount of drug released in almost a day, however, addition of HNT into zein matrix delayed the release of vancomycin 98% of the drug was released in 8 days. By looking at these two release profiles of drug in zein and zein-HNT matrix, the release rate is decreased due to the interaction between positive charge vancomycin with negative surface charge of HNTs as well as the increase of tortosity path of Vancomycin in zein matrix with the HNT addition (Pan et al., 2017). . In the case of drug loading into HNT nanotubes as a carrier of vancomycin, the fast initial release followed by a much slower release was achieved for both 1:2 and 1:5 vancomycin-HNTs ratios by diffusion through the tortuous path of nano clay HNTs as well as encapsulation of the drug in HNT nanotubes (Patel et al., 2016). Release profiles showed that cumulative drug release was 77,9% and 77,9% for 1:2 and 1:5 drug:HNT ratios for 14 days. Results showed that Vancomycin loaded HNT incorporated bilayer dressing prolonged the release rate up to 14 days. Avani and coworkers have studied release of vancomycin from only HNT nanotubes and they observed that nearly 50% of drug released in 500 hours (20 days) (Avani et al., 2019). . In another study, vancomycin release from HNTs studied and found that free vancomycin in a medium release in almost a day while cumulative release of 74,8 % for vancomycin loaded HNTs at pH 7 released in 5 weeks (35 days) (Pan et al., 2017).

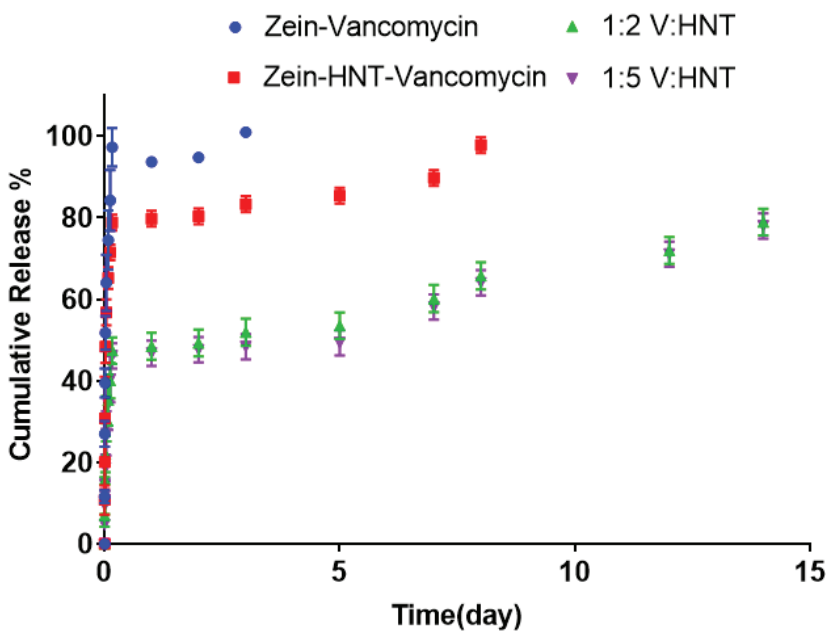

Figure 4. 21. Cumulative drug release of zein bilayer wound dressings.

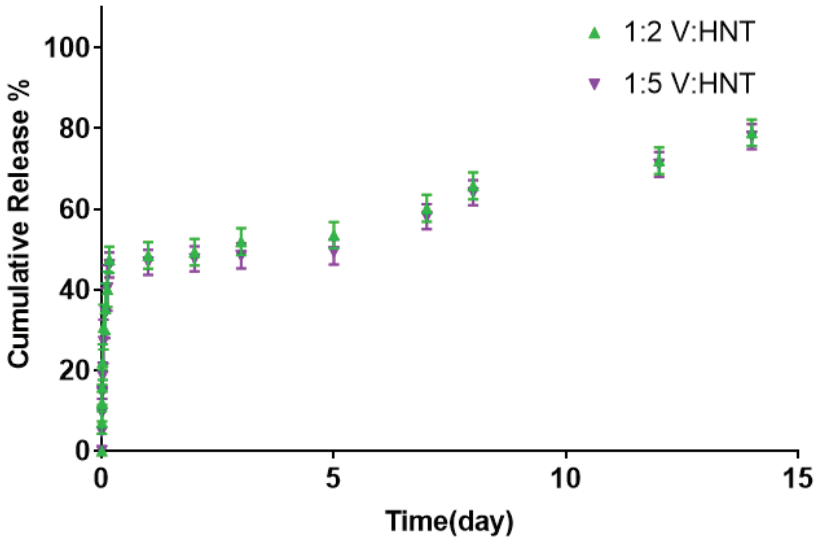

Figure 4. 22. Cumulative drug release from the bilayer dressing at different Vancomycin-HNT ratios (1:2, 1:5)

4.4.6. Kinetic Models

The release profile was examined by using different kinetic models as First-order, Higuchi, and Korsmeyer-Peppas models as explained in section 3.5.13 to determine the dominant kinetic model. Since the release profile showed initially burst release and then followed a sustained release, the cumulative drug release data was plotted by dividing them into two groups. According to cumulative release % first three hours was found burst release part which was noted as first region, and 3 hours to 14 days was second region representing as sustained release as shown in Figure 4.23, 4.24, 4.25 and Tables 4.13, 4.14. According to the R^2 values of different mathematical models, cumulative drug release profile fitted well to Higuchi kinetic model which had a highest average R^2 value of 0,98. Therefore, it can be said that the release profile was dominated by Higuchi release model. First order and Korsmeyer-Peppas models gave lower R^2 values than Higuchi model. This model is the most applied model in polymer release system. The mechanism of drug release was also determined by calculating n value in Korsmeyer-Peppas kinetic model which was found as 0,32. When considering the n value lower than 0.5 which was mentioned in early section in Table 3. 1. Fickian diffusion mechanism is the dominant mechanism for the release of the vancomycin drug.

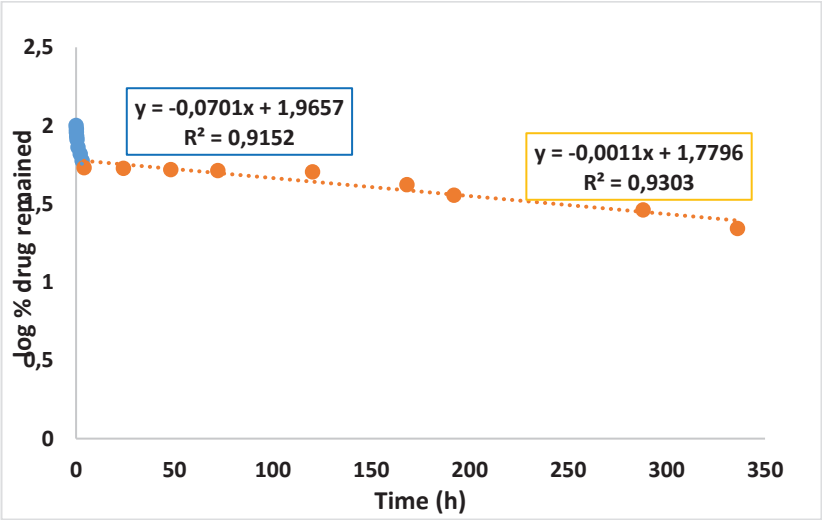

Figure 4. 23. First order kinetic model of Zein-drug loaded HNTs nanofibers

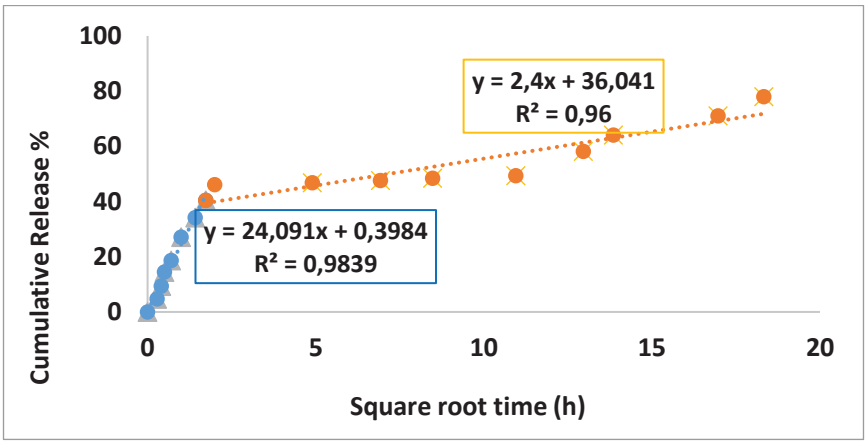

Figure 4. 24. Higuchi kinetic model of Zein-drug loaded HNTs nanofibers

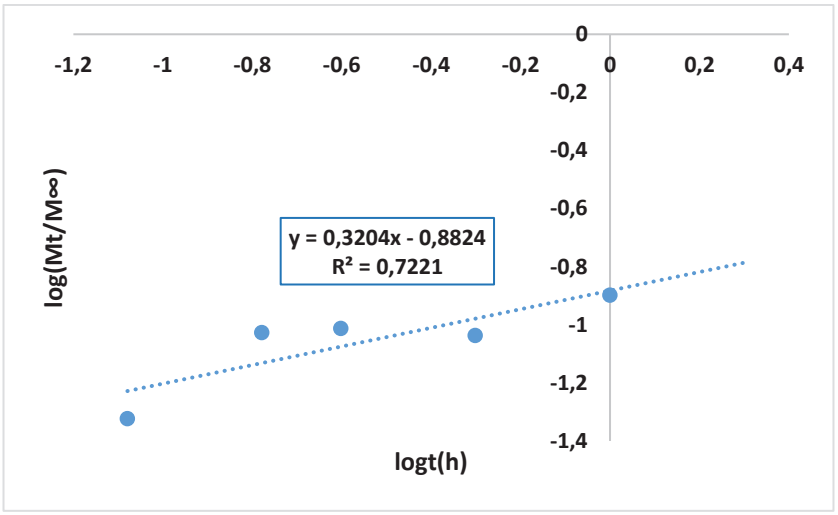

Figure 4. 25. Korsmeyer Peppas kinetic model of Zein-drug loaded HNTs nanofibers

Table 4. 13. R^2 values of First Order and Higuchi Kinetic models

1:5 Drug:HNT ratio	**First-order**	**Higuchi**
R^2 for burst release	0,91	0,98
k value for burst release	0,16	24,1
R^2 for sustained release	0,93	0,96
k value for sustained release	0,003	2,4

Table 4. 14. R^2 value and n value of Korsmeyer-Peppas Kinetic model

1:5 Drug:HNT ratio	**Korsmeyer-Peppas**
R^2 value	0,72
n value	0,32

4.4.7. Antimicrobial Test

For microbiological studies, the bilayer wound dressing consists of Vancomycin loaded Zein nanofiber (Drug:polymer ratio=1:5) on chitosan sponges was only investigated. Antimicrobial activity of release media of bilayer dressing at the end of 3 h and 24 h were tested on gram negative bacteria, *E.Coli* and gram positive bacteria*, S. epidermis* with in vitro media. As a result of disc diffusion test, it was seen that the wound dressings had an antimicrobial activity against *E. Coli* bacteria by using nutrient agar and tryptic soy agar. Zone areas were measured at the end of 24 h and 3 days and found as 1 mm, while control group (amoxicillin antibiotic disc) was noted as 7 mm zone diameter as seen from the images in Figure 4.26 and Table 4. 15 for gram negative and positive bacteria. The vancomycin antibiotic has a inhibition zone of 3 and 5 mm against *E.coli* and *S.Epidermidis* bacteria respectively compared to amoxicillin. The size of the inhibition diameter for our samples was found as similar in both agars. Antimicrobial activity continued for 3 days. However, when tests were applied against *S.epidermidis* microorganism, only bacterio static effect was observed while control group of vancomycin disc had 5 mm zone diameter.

Table 4. 15. Antibacterial Test for Control, 24h and 3 days drug release

	Control Group (Amoxillin)	**Vancomycin Antibiotic**	**Zone Diameter after 24h**	**Zone Diameter after 3 days**
E.Coli (tryptic soy agar)	7 mm	-	1 mm	1 mm
E.Coli (nutrient agar)	7 mm	3 mm	1 mm	1 mm
S.Epidermidis	10 mm	5 mm	Bacterio static effect	Bacterio static effect

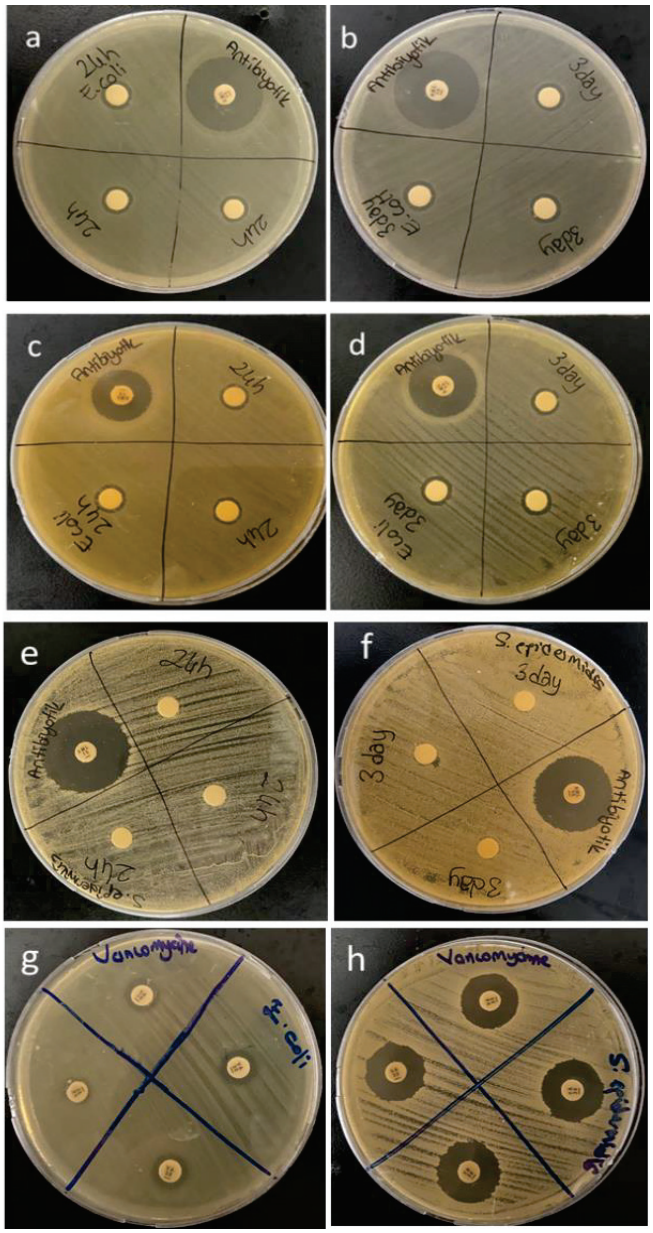

Figure 4. 26. Antimicrobial Test against *E.Coli* and *S.Epidermidis* (*E.Coli* nutrient agar with 24 h (a), 3 days release (b) and Vancomycin (g) ; E.coli tryptic soy agar with 24 h (c) 3 days release (d) ; *S.Epidermidis* with 24 h (e), 3 days release (f) and Vancomycin (h).

CHAPTER 5

CONCLUSION

Wound dressing applications have been improving from past to present. To make faster and efficient regeneration at the defect site of the skin, biomaterials were drawn attention recently. The most favorable wound dressings have homogeneous surface, high water uptake value to provide moist environment, low degradation, enough permeability to maintain moist, good antimicrobial activity and controlled drug release behavior. In the thesis, combination of zein-Vancomycin drug loaded HNTs electrospun nanofibers as upper layer with chitosan sponge as bottom layer was used to fabricate the bilayer membrane for wound dressing applications. The developed bilayer wound dressing mimic the ECM of skin due to its nanofiber layer & appropriate size and provide antibacterial protection against gram negative (E. coli) and positive (S. epidermidis) bacteria while providing gas transmission and absorbing excess exudates by the lower chitosan porous layer. In the study, Halloysite nanotubes were used as a carrier of antimicrobial agent. Vancomycin as model antibiotic that can be used against gram positive bacteria was encapsulated into HNT. HNTs can encapsulate multiple agents into tubes such as antibiotics, anti-corrosions and essential oils which makes drug release controlled and provide high mechanical and thermal behavior to the material. Initially Vancomycin is encapsulated into HNT, and then zein-vancomycin HNT is electrospun by electrospinning method. It was found that addition of different amount of HNTs (1,3 and 5 wt%) to zein nanofiber, mechanical behaviors increased, drug release profile slowed down, water uptake value increased, and material surface became more hydrophilic. Encapsulation of Vancomycin into HNTs was done by vacuum method. Encapsulation efficiency of drug loading was found as 23,35 % and 26,12 % for 1:2 and 1:5 Vancomycin: HNTs ratios respectively. The morphological characterization results of the upper layer showed that the electrospun nanofibers has 202,7± 0,05 – 225,2±0,06 nm fiber diameter which is found in the range of native skin tissue fibril diameters as between 50-500 nm. In addition, the lower layer consisting of chitosan, has a uniform porous structure with a 66,11 ± 0,96 % porosity. SEM images of the bilayer structure showed uniform coating of zein -drug loaded HNTs on the surface of porous chitosan layer. The bilayer membrane thickness was found 6850 μm. The bilayer wound dressings

also maintained sustained drug release up to 14 days with 77,97% and 77,91% of cumulative antibiotic release for both 1:2 and 1:5 drug: HNTs ratios. The release profile of antibiotics was fitted several models as First-order, Higuchi, and Korsmeyer-Peppas models. Among those, Higuchi Model, that is the most applied model for polymer release system, is found as the dominant release model with higher R^2 value. In addition, the bilayer dressing showed antimicrobial activity against *E. coli* and bacteriostatic effect for *S. Epidermis*. The water vapor transmission rate was found between 2833 and 2490 g/m^2day which is found in the appropriate range for wound healing. As a conclusion, zein and drug loaded HNTs nanofiber coated chitosan sponge bilayer mats as a novel composite wound dressing has promising properties to be used aa potential antimicrobial wound dressing applications.

REFERENCES

Adhirajan, Natarajan, Natesan Shanmugasundaram, Seetharaman Shanmuganathan, and Mary Babu. "Collagen-Based Wound Dressing for Doxycycline Delivery: In-Vivo Evaluation in an Infected Excisional Wound Model in Rats." *Journal of Pharmacy and Pharmacology* 61, no. 12 (2009): 1617-23.

Ali, Shamshad, Zeeshan Khatri, Kyung Wha Oh, Ick-Soo Kim, and Seong Hun Kim. "Zein/Cellulose Acetate Hybrid Nanofibers: Electrospinning and Characterization." *Macromolecular Research* 22, no. 9 (2014): 971-77.

Anisha, BS, Raja Biswas, KP Chennazhi, and R Jayakumar. "Chitosan–Hyaluronic Acid/Nano Silver Composite Sponges for Drug Resistant Bacteria Infected Diabetic Wounds." *International journal of biological macromolecules* 62 (2013): 310-20.

Avani, Farzaneh, Sheyda Damoogh, Fatemeh Mottaghitalab, Akbar Karkhaneh, and Mehdi Farokhi. "Vancomycin Loaded Halloysite Nanotubes Embedded in Silk Fibroin Hydrogel Applicable for Bone Tissue Engineering." *International Journal of Polymeric Materials and Polymeric Biomaterials* (2019).

Babu, Mary. "Collagen Based Dressings—a Review." *Burns* 26, no. 1 (2000): 54-62.

Bharathi, SK Vimala, M Maria Leena, JA Moses, and C Anandharamakrishnan. "Zein Based Anti-Browning Cling Wraps for Fresh Cut Apple Slices." *International Journal of Food Science & Technology* (2019).

Boateng, Joshua S, Kerr H Matthews, Howard NE Stevens, and Gillian M Eccleston. "Wound Healing Dressings and Drug Delivery Systems: A Review." *Journal of pharmaceutical sciences* 97, no. 8 (2008): 2892-923.

Cui, Gan, Zhenxiao Bi, Shuaihua Wang, Jianguo Liu, Xiao Xing, Zili Li, and Bingying Wang. "A Comprehensive Review on Smart Anti-Corrosive Coatings." *Progress in Organic Coatings* 148 (2020): 105821.

Cui, Jing, Liying Qiu, Yuyu Qiu, Qingqing Wang, and Qufu Wei. "Co-Electrospun Nanofibers of Pva-Sbq and Zein for Wound Healing." *Journal of Applied Polymer Science* 132, no. 39 (2015).

Dashdorj, Uyanga, Mark Kenneth Reyes, Afeesh Rajan Unnithan, Arjun Prasad Tiwari, Batgerel Tumurbaatar, Chan Hee Park, and Cheol Sang Kim. "Fabrication and Characterization of Electrospun Zein/Ag Nanocomposite Mats for Wound Dressing Applications." *International journal of biological macromolecules* 80 (2015): 1-7.

de Oliveira, A. D., & Beatrice, C. A. G. "Polymer Nanocomposites with Different Types of Nanofiller." *In Nanocomposites-Recent Evolutions* (2018): IntechOpen.

Debra, JB, and O Cheri. "Wound Healing: Technological Innovations and Market Overview." *Technology Catalysts International Corporation* 2 (1998): 1-185.

Değer, S. "Preparation and characterization of herbal extract loaded bilayer sponges for wound dressing applications". Izmir Institute of Technology, (2019).

Deshmukh, K, M Basheer Ahamed, RR Deshmukh, SK Khadheer Pasha, PR Bhagat, and K Chidambaram. "Biopolymer Composites with High Dielectric Performance: Interface Engineering." In *Biopolymer Composites in Electronics*, 27-128: Elsevier, 2017.

Dhivya, Selvaraj, Viswanadha Vijaya Padma, and Elango Santhini. "Wound Dressings–a Review." *BioMedicine* 5, no. 4 (2015): 1-5.

Dong, Yu, Jordan Marshall, Hazim J Haroosh, Soheila Mohammadzadehmoghadam, Dongyan Liu, Xiaowen Qi, and Kin-Tak Lau. "Polylactic Acid (Pla)/Halloysite Nanotube (Hnt) Composite Mats: Influence of Hnt Content and Modification." *Composites Part A: Applied Science and Manufacturing* 76 (2015): 28-36.

El Ashram, S., El-Samad, L. M., Basha, A. A., & El Wakil, A. "Naturally-derived targeted therapy for wound healing: Beyond classical strategies." *Pharmacological Research*, (2021):105749.

Feitosa, SA, J Palasuk, K Kamocki, S Geraldeli, RL Gregory, JA Platt, LJ Windsor, and MC Bottino. "Doxycycline-Encapsulated Nanotube-Modified Dentin Adhesives." *Journal of dental research* 93, no. 12 (2014): 1270-76.

Georget, D. M., Barker, S. A., & Belton, P. S. "A study on maize proteins as a potential new tablet excipient." *European Journal of Pharmaceutics and Biopharmaceutics*, 69(2), (2008): 718-726.

Ghomi, E. R., S. Khalili, S. N. Khorasani, R. E. Neisiany, and S. Ramakrishna. "Wound Dressings: Current Advances and Future Directions." *Journal of Applied Polymer Science* 136, no. 27 (Jul 2019): 47738.

Ghorbani, Marjan, Parinaz Nezhad-Mokhtari, and Soghra Ramazani. "Aloe Vera-Loaded Nanofibrous Scaffold Based on Zein/Polycaprolactone/Collagen for Wound Healing." *International journal of biological macromolecules* 153 (2020): 921-30.

Gorrasi, Giuliana, and Luigi Vertuccio. "Evaluation of Zein/Halloysite Nano-Containers as Reservoirs of Active Molecules for Packaging Applications: Preparation and Analysis of Physical Properties." *Journal of Cereal Science* 70 (2016): 66-71.

Grace, Edward. "Altered Vancomycin Pharmacokinetics in Obese and Morbidly Obese Patients: What We Have Learned over the Past 30 Years." *Journal of Antimicrobial Chemotherapy* 67, no. 6 (2012): 1305-10.

Gunes, Seda, Sedef Tamburaci, and Funda Tihminlioglu. "A Novel Bilayer Zein/Mmt Nanocomposite Incorporated with H. Perforatum Oil for Wound Healing." *Journal of Materials Science: Materials in Medicine* 31, no. 1 (2020): 1-19.

Ikeda, Takeshi, Kahori Ikeda, Kouhei Yamamoto, Hidetaka Ishizaki, Yuu Yoshizawa, Kajiro Yanagiguchi, Shizuka Yamada, and Yoshihiko Hayashi. "Fabrication and Characteristics of Chitosan Sponge as a Tissue Engineering Scaffold." *BioMed research international* 2014 (2014).

Jayakumar, R., Prabaharan, M., Kumar, P. S., Nair, S., & Tamura, H. "Biomaterials based on chitin and chitosan in wound dressing applications." *Biotechnology advances*, 29(3), (2011): 322-337.

Johnson, Jennifer LH, and Samuel H Yalkowsky. "Reformulation of a New Vancomycin Analog: An Example of the Importance of Buffer Species and Strength." *AAPS PharmSciTech* 7, no. 1 (2006): E33-E37.

Kalra, A., Lowe, A., & Al-Jumaily, A. "Mechanical behaviour of skin: a review." J. Mater. Sci. Eng, 5(4), (2016): 1000254.

Kayaci, Fatma, and Tamer Uyar. "Electrospun Zein Nanofibers Incorporating Cyclodextrins." *Carbohydrate polymers* 90, no. 1 (2012): 558-68.

Kimna, Ceren, Sedef Tamburaci, and Funda Tihminlioglu. "Novel Zein-Based Multilayer Wound Dressing Membranes with Controlled Release of Gentamicin." *Journal of Biomedical Materials Research Part B: Applied Biomaterials* (2018).

Kolarsick, Paul A. J., Maria Ann Kolarsick, and Carolyn Goodwin. "Anatomy and Physiology of the Skin." *Journal of the Dermatology Nurses' Association* 3, no. 4 (2011): 203-13.

Kurtoglu, Aslıhan Hilal, and Ayşegül Karatas. "Yara Tedavisinde Güncel Yaklaşımlar: Modern Yara Örtüleri." (2009).

Lee, Hoik, Gang Xu, Davood Kharaghani, Masayoshi Nishino, Kyung Hun Song, Jung Soon Lee, and Ick Soo Kim. "Electrospun Tri-Layered Zein/Pvp-Go/Zein Nanofiber Mats for Providing Biphasic Drug Release Profiles." *International journal of pharmaceutics* 531, no. 1 (2017): 101-07.

Lee, Min Hyeock, Hyun-Sun Seo, and Hyun Jin Park. "Thyme Oil Encapsulated in Halloysite Nanotubes for Antimicrobial Packaging System." *Journal of food science* 82, no. 4 (2017): 922-32.

Lin, Jiantao, Caihong Li, Yi Zhao, Jianchan Hu, and Li-Ming Zhang. "Co-Electrospun Nanofibrous Membranes of Collagen and Zein for Wound Healing." *ACS applied materials & interfaces* 4, no. 2 (2012): 1050-57.

Liu, Jia-Xu, Wen-Hao Dong, Xiao-Ju Mou, Guo-Sai Liu, Xiao-Wei Huang, Xu Yan, Cheng-Feng Zhou, Shouxiang Jiang, and Yun-Ze Long. "In Situ Electrospun Zein/Thyme Essential Oil-Based Membranes as an Effective Antibacterial Wound Dressing." *ACS Applied Bio Materials* 3, no. 1 (2019): 302-07.

Losquadro, William D. "Anatomy of the Skin and the Pathogenesis of Nonmelanoma Skin Cancer." *Facial Plast Surg Clin North Am* 25, no. 3 (2017): 283-89.

Luo, Yangchao, and Qin Wang. "Zein-Based Micro-and Nano-Particles for Drug and Nutrient Delivery: A Review." *Journal of Applied Polymer Science* 131, no. 16 (2014).

Lvov, Yuri, and Elshad Abdullayev. "Functional Polymer–Clay Nanotube Composites with Sustained Release of Chemical Agents." *Progress in Polymer Science* 38, no. 10-11 (2013): 1690-719.

Mariotti, C. E., Ramos-Rivera, L., Conti, B., & Boccaccini, A. R. "Zein-based electrospun fibers containing bioactive glass with antibacterial capabilities." *Macromolecular Bioscience*, 20(7), (2020): 2000059.

Martin, Paul, and R Nunan. "Cellular and Molecular Mechanisms of Repair in Acute and Chronic Wound Healing." *British Journal of Dermatology* 173, no. 2 (2015): 370-78.

Memic, Adnan, Tuerdimaimaiti Abudula, Halimatu S Mohammed, Kasturi Joshi Navare, Thibault Colombani, and Sidi A Bencherif. "Latest Progress in Electrospun Nanofibers for Wound Healing Applications." *ACS Applied Bio Materials* 2, no. 3 (2019): 952-69.

Miguel, S. P., Moreira, A. F., & Correia, I. J. "Chitosan based-asymmetric membranes for wound healing: A review." *International journal of biological macromolecules,* 127, (2019): 460-475.

Moore, Zena EH, and Joan Webster. "Dressings and Topical Agents for Preventing Pressure Ulcers." *Cochrane Database of Systematic Reviews*, no. 12 (2018).

Morgado, Patrícia I, Pedro F Lisboa, Maximiano P Ribeiro, Sónia P Miguel, Pedro C Simões, Ilídio J Correia, and Ana Aguiar-Ricardo. "Poly (Vinyl Alcohol)/Chitosan Asymmetrical Membranes: Highly Controlled Morphology toward the Ideal Wound Dressing." *Journal of membrane science* 469 (2014): 262-71.

Ndlovu, S. P., Ngece, K., Alven, S., & Aderibigbe, B. A. "Gelatin-Based Hybrid Scaffolds: Promising Wound Dressings. Polymers," 13(17), (2021): 2959.

Nilsen-Nygaard, J., Strand, S. P., Vårum, K. M., Draget, K. I., & Nordgård, C. T. "Chitosan: gels and interfacial properties." *Polymers*, 7(3), (2015): 552-579.

Ong, Shin-Yeu, Jian Wu, Shabbir M Moochhala, Mui-Hong Tan, and Jia Lu. "Development of a Chitosan-Based Wound Dressing with Improved Hemostatic and Antimicrobial Properties." *Biomaterials* 29, no. 32 (2008): 4323-32.

Pan, Qingqing, Neng Li, Yu Hong, Heng Tang, Zongfu Zheng, Shaohuang Weng, Yanjie Zheng, and Liying Huang. "Halloysite Clay Nanotubes as Effective Nanocarriers for the Adsorption and Loading of Vancomycin for Sustained Release." *RSC advances* 7, no. 34 (2017): 21352-59.

Patel, DK, A Biswas, and P Maiti. "Nanoparticle-Induced Phenomena in Polyurethanes." In *Advances in Polyurethane Biomaterials*, 171-94: Elsevier, 2016.

Patel, Satish, Shikha Srivastava, Manju Rawat Singh, and Deependra Singh. "Preparation and Optimization of Chitosan-Gelatin Films for Sustained Delivery of Lupeol for Wound Healing." *International journal of biological macromolecules* 107 (2018): 1888-97.

Pavliňáková, Veronika, Zdenka Fohlerová, David Pavliňák, Viera Khunová, and Lucy Vojtová. "Effect of Halloysite Nanotube Structure on Physical, Chemical, Structural and Biological Properties of Elastic Polycaprolactone/Gelatin Nanofibers for Wound Healing Applications." *Materials Science and Engineering: C* 91 (2018): 94-102.

Quek, Siew Young, Joshua Hadi, and Hartono Tanambell. "Application of Electrospinning as Bioactive Delivery System." (2019).

Rad, Zahra Pedram, Javad Mokhtari, and Marjan Abbasi. "Fabrication and Characterization of Pcl/Zein/Gum Arabic Electrospun Nanocomposite Scaffold for Skin Tissue Engineering." *Materials Science and Engineering: C* 93 (2018): 356-66.

Ramos-e-Silva, Marcia, and Maria Cristina Ribeiro de Castro. "New Dressings, Including Tissue-Engineered Living Skin." *Clinics in dermatology* 20, no. 6 (2002): 715-23.

Shi, Chenyu, Chenyu Wang, He Liu, Qiuju Li, Ronghang Li, Yan Zhang, Yuzhe Liu, Ying Shao, and Jincheng Wang. "Selection of Appropriate Wound Dressing for Various Wounds." *Frontiers in bioengineering and biotechnology* 8 (2020): 182.

Shi, Rui, Yuzhao Niu, Min Gong, Jingjing Ye, Wei Tian, and Liqun Zhang. "Antimicrobial Gelatin-Based Elastomer Nanocomposite Membrane Loaded with Ciprofloxacin and Polymyxin B Sulfate in Halloysite Nanotubes for Wound Dressing." *Materials Science and Engineering: C* 87 (2018): 128-38.

Sofokleous, P., Stride, E., Bonfield, W., & Edirisinghe, M. "Design, construction and performance of a portable handheld electrohydrodynamic multi-needle spray gun for biomedical applications." *Materials Science and Engineering*: C, 33(1), (2013): 213-223.

Tamburaci, Sedef, and Funda Tihminlioglu. "Development of Si Doped Nano Hydroxyapatite Reinforced Bilayer Chitosan Nanocomposite Barrier Membranes for Guided Bone Regeneration." *Materials Science and Engineering: C* 128 (2021): 112298.

Tamburaci, Sedef, and Funda Tihminlioglu. "Novel Poss Reinforced Chitosan Composite Membranes for Guided Bone Tissue Regeneration." *Journal of Materials Science: Materials in Medicine* 29, no. 1 (2018): 1-14.

Thomas, S., Loveless, P., & Hay, N. "Comparative review of the properties of six semipermeable film dressings." *Pharm J*, 240, (1988): 785-787.

Thu, Hnin-Ei, Mohd Hanif Zulfakar, and Shiow-Fern Ng. "Alginate Based Bilayer Hydrocolloid Films as Potential Slow-Release Modern Wound Dressing." *International journal of pharmaceutics* 434, no. 1-2 (2012): 375-83.

Ueno, Hiroshi, Haruo Yamada, Ichiro Tanaka, Naoki Kaba, Mitsunobu Matsuura, Masahiro Okumura, Tsuyoshi Kadosawa, and Toru Fujinaga. "Accelerating Effects of Chitosan for Healing at Early Phase of Experimental Open Wound in Dogs." *Biomaterials* 20, no. 15 (1999): 1407-14.

Ullah, Sana, Motahira Hashmi, Muhammad Qamar Khan, Davood Kharaghani, Yuseke Saito, Takayuki Yamamoto, and Ick Soo Kim. "Silver Sulfadiazine Loaded Zein Nanofiber Mats as a Novel Wound Dressing." *RSC advances* 9, no. 1 (2019): 268-77.

Wali, A., Gorain, M., Inamdar, S., Kundu, G., & Badiger, M. "In vivo wound healing performance of halloysite clay and gentamicin-incorporated cellulose ether-PVA electrospun nanofiber mats." *ACS Applied Bio Materials*, 2(10), (2019): 4324-4334.

Yilmaz, Refik Baris, Goknur Bayram, and Ulku Yilmazer. "Effect of Halloysite Nanotubes on Multifunctional Properties of Coaxially Electrospun Poly (Ethylene Glycol)/Polyamide-6 Nanofibrous Thermal Energy Storage Materials." *Thermochimica Acta* 690 (2020): 178673.

Yu, Yi-Hsun, Demei Lee, Yung-Heng Hsu, Ying-Chao Chou, Steve WN Ueng, Che-Kang Chen, and Shih-Jung Liu. "A Three-Dimensional Printed Polycaprolactone Scaffold Combined with Co-Axially Electrospun Vancomycin/Ceftazidime/Bone Morphological Protein-2 Sheath-Core Nanofibers for the Repair of Segmental Bone Defects During the Masquelet Procedure." *International journal of nanomedicine* 15 (2020): 913.

Yuan, Y., Hays, M. P., Hardwidge, P. R., & Kim, J. "Surface characteristics influencing bacterial adhesion to polymeric substrates." *RSC advances*, 7(23), (2017): 14254-14261.

Zahedi, Payam, Iraj Rezaeian, Seyed-Omid Ranaei-Siadat, Seyed-Hassan Jafari, and Pitt Supaphol. "A Review on Wound Dressings with an Emphasis on Electrospun Nanofibrous Polymeric Bandages." *Polymers for Advanced Technologies* 21, no. 2 (2010): 77-95.

Zare, M., Dziemidowicz, K., Williams, G. R., & Ramakrishna, S. "Encapsulation of pharmaceutical and nutraceutical active ingredients using electrospinning processes." *Nanomaterials*, 11(8), (2021): 1968.

Zheng, Yueyuan, Yuqing Liang, Depan Zhang, Xiaoyi Sun, Li Liang, Juan Li, and You-Nian Liu. "Gelatin-Based Hydrogels Blended with Gellan as an Injectable Wound Dressing." *ACS omega* 3, no. 5 (2018): 4766-75.

Zou, Yucheng, Cen Zhang, Peng Wang, Yipeng Zhang, and Hui Zhang. "Electrospun Chitosan/Polycaprolactone Nanofibers Containing Chlorogenic Acid-Loaded Halloysite Nanotube for Active Food Packaging." *Carbohydrate Polymers* 247 (2020): 116711.

APPENDIX A

VANCOMYCIN CALIBRATION CURVE

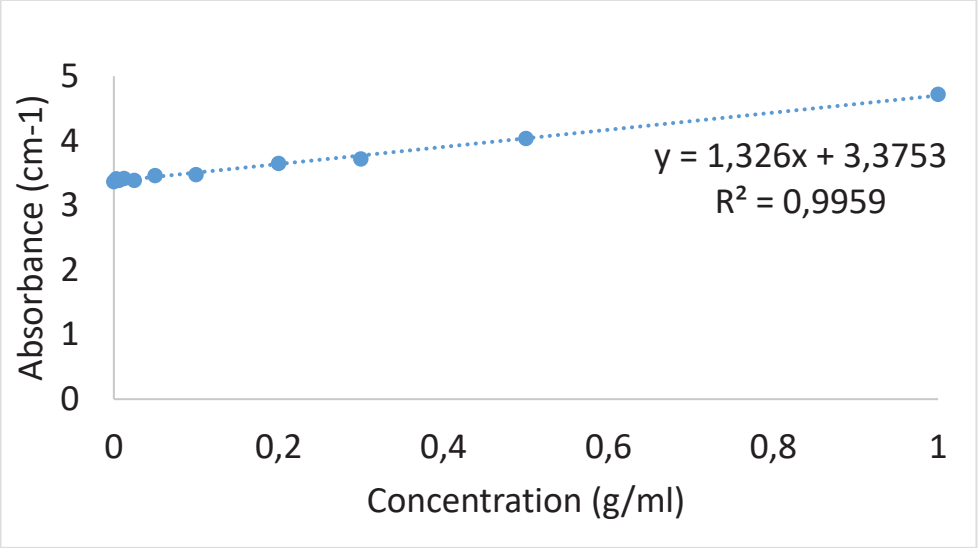

Figure A.1. Vancomycin calibration curve graph

APPENDIX B

AFM IMAGE OF HNT

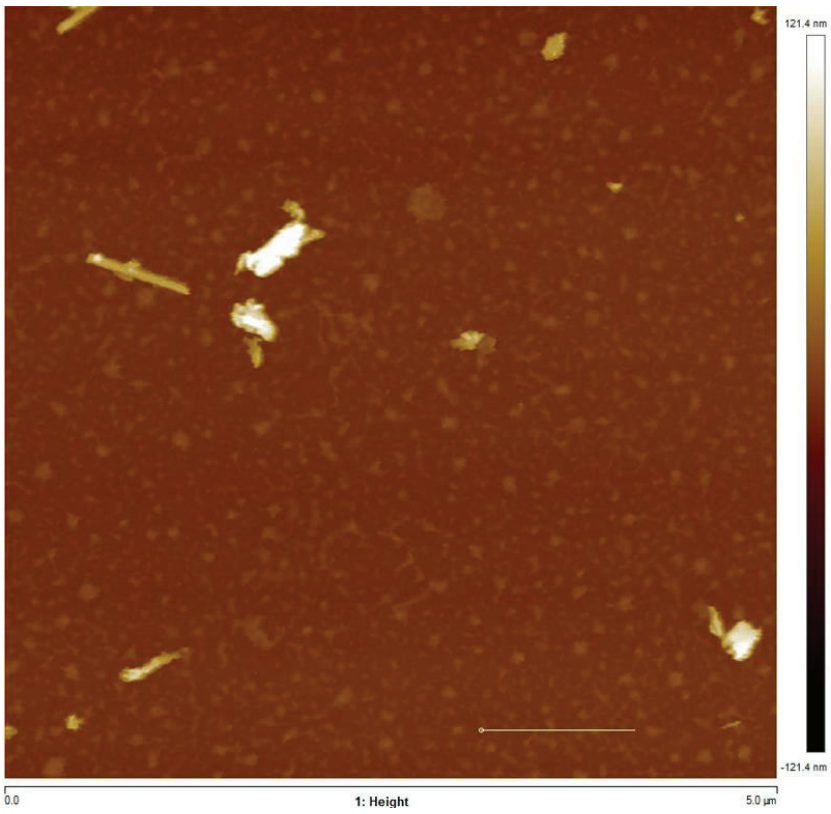

Figure B.1. AFM Image of HNT (Scale bar 120nm)